Results: We used NSCLC cell lines to verify that the mutation-specific antibodies can specifically detect EGFR mutations and the EpCAM antibody was selectively labeled at the epithelial cells by fluorescence immunocytochemistry.

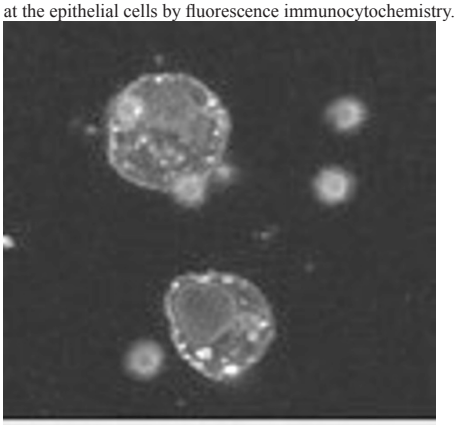

Next, we tested the cancer cell lines enriched from mixed with blood.

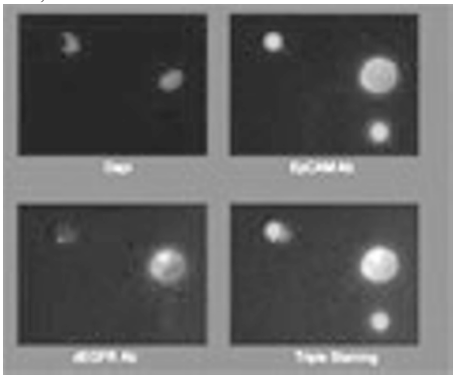

Finally, we confirmed the assay from the cells recovered from the blood or pleural effusion of late stage NSCLC patients.

Conclusions: Fluorescence immunocytochemistry with mutation-specific antibodies to detect EGFR mutations on the tumor cells from blood or pleural effusion is a reliable, easily accessible and cost efficient assay for patient selective to target therapy, especially in the late stage NSCLC patients without tumor tissue or the patients treated by TKI for following up the response.

1916 Protein Expression Profiling of Irinotecan Pathway in Lung Cancer

W Zhang, WS Zhang, EL Lee, HL McLeod. Howard University Hospital, Washington, DC; The Second Hospital of Nanjing, Nanjing, Jiangsu, China; UNC School of Pharmacy, Chapel Hill, NC.

Background: The exact mechanism for variation of response to chemotherapy remains unclear. Individualized therapy strategies for cancer will require a more thorough understanding of the pathways influencing drug fate, including expression of cellular target enzymes, metabolism enzymes and cellular transporters. Irinotecan is an excellent example of an anticancer drug in need of individualization. We profile expression of proteins in an irinotecan pathway in lung small cell carcinoma and non-small cell carcinoma tissues and construct a new pharmacologic pathway to help advance individualization in the selection of cancer therapy.

Design: Paraffin embedded tumor tissues from 15 patients with lung small cell carcinoma, 49 patients with stage IV non-small cell carcinoma (21 squamous cell carcinoma, 18 adenocarcinoma and 10 undifferentiated large cell carcinoma) were used to construct a tissue microarray. Fifteen markers, including CES2, NFkappaB, XRCC1, CDC45, TDP1, TOP1, PARP1, ABCC1, ABCC2, ABCC3, ABCB1, ABCG2, p53, ERCC2, UGT1A1, that are related to the irinotecan pathway were immunohistochemically stained on the tissue microarray. Protein expression was assessed to derive an overall expression level. Hierarchical clustering was used with unsupervised algorithms to identify patterns of protein expression that produced distinct clusters of patients.

Results: The relative expression levels across the 15 pathway proteins and the interpatient variability were considerable. Using hierarchical clustering, 4 protein clusters and 3 patient groups had highly similar indices based on the protein expressions. Protein expression of this drug pathway is not associated with lung carcinoma histological type. Cluster analysis identified a variety of histological types with the same pharmacological profile. The 3 patient groups had no unique clinical pathologic features but could be differentiated by the statistically significant differences in the protein expression levels of 5 proteins.

Conclusions: Gene expression profiling could be valuable for predicting tumor response to chemotherapy and for tailoring therapy to individual cancer patients. Establishing the ability of pathway analysis to discern patient populations who have a high likelihood of benefit from a given chemotherapy agent or those who will receive no benefit will provide the basis for selection of therapy for individual patients.

1917 Discovering Multivariate Gene Expression Markers for Relapse Prediction in Pediatric Acute Lymphoblastic Leukemia

Y Zhou, D Dziuda. New York Medical College, Valhalla, NY; Central Connecticut State University, New Britain, CT.

Background: Identification of cancer patients with high risk of treatment failure is becoming an important aspect of pathology practice. Discovery of reliable predictive and prognostic markers using high content gene expression profiling or genome analysis have proven both promising and challenging. Oncogenesis is a result of heterogeneous signaling dysregulation converged on critical cellular functions. The goal in discovery of predictive and prognostic marker is to identify a minimal set of genes or proteins that has maximal discriminating power to separate phenotypic classes, and reveals the underlying mechanism contributing to the phenotypic differences.

Design: We describe a supervised multivariate biomarker discovery approach utilizing stepwise selection driven by a well-defined measure of discriminatory power (the Lawley-Hotelling T 2 metric), which (i) allows for identification of a set of genes whose joint expression pattern efficiently discriminate phenotypic classes, (ii) facilitates biological interpretation of underlying dysregulations. This approach is illustrated on prediction of relapse in pediatric B-cell acute lymphoblastic leukemia (B-cell ALL) using publicly available gene expression data sets.

Results: Based on a cohort of B-cell ALL with mixed subtypes of cytogenetic changes, a set of genes, less than 20, was identified as a multivariate biomarker for predicting the risk of disease relapse. This marker is then tested on another independent set of B-cell ALL, and predicts disease relapse with 91% sensitivity. Ensemble of the biomarker reveals gene expression pattern that is associated with the relapse risk in B-cell ALL.

Conclusions: We demonstrate the usefulness of multivariate approach in identifying a small set of prognostic marker. The marker contains sufficiently small numbers of genes that can be readily converted to RT-PCR based assays.

Techniques

1918 Biospecimen Inventory and Operations System (BIOS) for Management of Annotated Tissue Bank Specimens for Anatomical Pathology

W Amin, G Greenwood, M Bisceglia, L Mock, R Dhir, AV Parwani. University of Pittsburgh, Pittsburgh, PA; University of Pittsburgh Medical Center, Pittsburgh, PA.

Background: There is a need for tools that provide researchers access to highly annotated biospecimens for research. The Biospecimen Inventory and Operations System is an enterprise biorepository system designed for a high-quality, well annotated biospecimen management for clinician and researchers need. It provides a robust query capability that eventually allows biomarkers to identify the biospecimens as per the need of the research community.

Design: BIOS is a Microsoft .NET web application with a SQL Server database. It unifies the efforts of tissue collection, patient consents status, billing and data aggregation in one module. It links to Medipac for accurate importing of patient demographics. It will pull patient mapped data automatically through integration with lab information systems and synoptics and other institutional electronic data sources, from hospital information systems.

Results: The BIOS system has been successfully implemented at our institute and is currently being used for the day to day operations of a system-wide tissue bank. BIOS provides a central repository for the tissue bankers for tracking and distribution of biospecimens and for robust querying and reporting of biospecimens and associated data to fulfill the requirements of clinical translational researchers. By combining the flexible query interface of BIOS with the ability to export the result of queries, the tissue bankers will be able to prepare virtually any custom report they require, from summaries of bank-wide operations during a specified period to daily work lists for a particular banker.

Conclusions: BIOS in provides a central biorepository to access information on multimodal data sets and the ability for tracking and integration with other limbs of a tissue bank. In addition BIOS provides the tissue bankers with a robust, queryable, and maintainable system that can be integrated with other tissue banking and pathology tools including image and molecular data integration. Furthermore, this model can be successfully deployed at other institutions.

1919 Standard PCR Sequencing Underestimates KRAS and BRAF Mutations in Advanced Colorectal Carcinomas: Comparison with LNA-Modified PCR Sequencing and Sequenom Mass Spectrometry Genotyping

ME Arcila, CY Lau, K Nafa, M Ladanyi. Memorial Sloan Kettering Cancer Center, New York.

Background: KRAS and BRAF mutations are associated with primary resistance to epidermal growth factor receptor (EGFR) inhibitors and, together, are identified in about 50% of patients with advanced colorectal carcinoma. Mutation screening can therefore be used to identify a large proportion of patients who are unlikely to respond to this therapy. Detecting mutations in this setting can be challenging, particularly when testing volume is high and based on samples with a low proportion of tumor cells which, if below 25%, may not be reliably detected by standard sequencing. To address these issues, we designed and evaluated two assays - a locked nucleic acid (LNA)-based PCR-sequencing assay, to allow the detection of low levels of mutant DNA and a Sequenom MALDI-TOF mass spectrometry-based genotyping assay, suitable for large scale mutation screening.

Design: Clinical cases consecutively tested for KRAS exon 2 and BRAF exon 15 mutations by standard sequencing (with microdissection as needed) were retested with modified PCR and sequencing, using standard primers and a 10-mer LNA oligonucleotide designed to suppress amplification of non-mutant DNA. Samples were also tested using a Sequenom assay targeting the most common mutations in both genes.

Results: We tested 308 tumor samples by all 3 methods. Initial testing using standard sequencing detected 121 KRAS (39%) and 10 BRAF mutations, for a combined 42.5%. Retesting with the LNA-based method and the Sequenom assay detected 20 (141/308, 46%) and 4 (125/308, 41%) additional KRAS mutants, respectively. One additional BRAF mutant was detected by the Sequenom assay only, for a combined KRAS/BRAF proportion of 49.4% for the two new assays. The analytical sensitivity of the LNA-modified method, based on serial dilutions of mutant and normal control DNA, is below 0.3% for both KRAS and BRAF. The analytical sensitivity of the Sequenom assay ranged from 1-10% depending on the mutation tested.

Conclusions: The technical sensitivity of the LNA-PCR sequencing assay is well beyond that of standard PCR-sequencing and is particularly useful in the testing of specimens not amenable to pre-dissection due to a diffuse infiltrative pattern without discrete tumor nests. The Sequenom assay has an intermediate sensitivity but offers significant advantages for large scale mutation screening. Standard sequencing (even with microdissection) may miss approximately 14% (49.4%-42.5% /49.4%) of patients resistant to EGFR antibody therapy.

1920 *NPM1* Mutation Detection: A Comparative Study of Quantitative Real-Time PCR and Capillary Electrophoresis in 157 Clinical Samples

FH Barakat, R Luthra, LJ Medieros, BA Barkoh, J Li, S Hai, W Jamil, YI Bhakta, S Herrmann, SS Chen, Z Zuo. MD Anderson Cancer Center, Houston, TX.

Background: Nucleophosmin (*NPM1*) is one of the most commonly mutated genes in acute myeloid leukemia (AML) and has prognostic significance. The presence of *NPM1* mutation predicts a better prognosis in AML patients, particularly in the subgroup with diploid cytogenetics and no evidence of *FLT3* gene mutation. *NPM1* mutations involve exon 12 and cause a frame shift in the translation and aberrant cytoplasmic dislocation of NPM1 protein. Most of these mutations involve a 4-bp insertion in a limited region, which can be detected by capillary electrophoresis (CE) or by real-time quantitative PCR (RQ-PCR) methods. besides its prognostic importance, *NPM1* mutation can be helpful in monitoring minimal residual disease (MRD).

Design: This study compared CE and RQ-PCR, for assessing for NPM1 mutation in peripheral blood or marrow samples of 157 patients sent for NPM1 study. Our laboratory currently uses CE assay as routine test. For this study, we developed a multiplex RQ-PCR assay using single TaqMan probe and 6 mutation-specific primers to detect the most common *NPM1* mutations, accounting for >95% of cases. This RQ-PCR method was run parallel with our CE assay. Analytical sensitivities of both methods were determined by serial dilution studies. Different mutation types and discordant results between the two methods were further validated by Sanger sequencing.

Results: Serial dilution studies showed that the RQ-PCR method has mutation detection sensitivity of higher than 1:100 cells, compared with approximately 1:40 cells for the CE method. The RQ-PCR assay involves only one step, unlike the two-step CE method, and therefore turn-around time was also cut in half using RQ-PCR. Among the 157 clinical samples tested, 155 (98.7%) showed concordant results. Two samples were discordant: 1 RQ-PCR+ and CE- and 1 RQ-PCR- and CE+. Sanger sequencing analysis in both cases was negative. Given the fact that the sensitivities of both assays are well above that of Sanger sequencing, we are unable to use Sanger sequencing to determine whether these two cases were true or false positives. Within this study cohort, frequency of *NPM1* and *FLT3* mutation was 19% and 23% in AML, respectively, and 7% and 0% in MDS, respectively.

Conclusions: The RQ-PCR method developed here generated highly concordant results compared with our CE assay for *NPM1* mutation detection. In addition, the RQ-PCR assay is more sensitive, rapid and cost effective, making it ideal for monitoring MRD.

1921 Use of Whole Slide Digital Images for Determination of Ki-67 (MIB-1) Labeling Index in Infiltrating Astrocytomas: Comparison of Current Counting Methods with an Image-Based Algorithm

M Bonham, R Monroe, R Allen, M Almaula, T Tihan. University of California, San Francisco, CA; Bioimagene, Sunnyvalle, CA.

Background: While mitotic rates as well as proliferation indices have been reported as significantly different among different grades of infiltrating astrocytomas, a reproducible cut-off value has not emerged. The goal of this study was to determine whether more reproducible algorithms using whole slide digital images (WSDI) can define better cut-off values for different grades of infiltrating astrocytomas.

Design: Whole tissue sections from 35 infiltrating astrocytomas grades II through IV were evaluated to determine the best slides/blocks for Mib1 immunohistochemistry. 1000 cells were manually counted for MIB1 positivity. The same slides were then used for WSDI. The slides were scanned using the iScan™ automated whole slide scanning system and were viewed using the ImageViewer™. Single fields of view (FOV) from each WSDI measuring ~420,000 μ^2 that represented the highest density of Ki-67 positive nuclei were selected for image analysis. Three different FOVs were analyzed in a subset of slides to determine the variability in each case. The total Ki-67 labeling index as well as average surface area of positive and negative tumor cells were calculated in MatLab™.

Results: We analyzed labeling indices in 13 grade II, 6 grade III and 16 grade IV astrocytomas using both methods. The mean labeling indices for manual and automated counts were 2.4 and 2.6 for grade II tumors, 10.3 and 12.4 for grade III and 15.8 and 20.9 for grade IV tumors, respectively. The correlation coefficients between manual and automated counts were 0.79 for grade II, 0.86 for grade III, and 0.79 for grade IV astrocytomas. The overall correlation coefficient for the entire series was 0.87. In addition, the mean nuclear area for positive cells was 92.2 μ^2 for grade II, 102.2 μ^2 for grade III and 86.8 μ^2 for grade IV astrocytomas. Analysis of three different FOVs per slide yielded a correlation coefficient of 0.87 when compared to analysis of a single separate FOV.

Conclusions: Our analysis yielded a similarly increasing labeling index for astrocytoma grades II through IV using both methods. Additional information such as the mean size of tumor nuclei was obtained for WSDI. Both counting methods still suffer from a sampling bias due to subjective selection of the area to be counted. Developing optimal algorithms based on tissue and tumor type may be more reproducible in predicting the value of proliferation indices in CNS neoplasms.

1922 Use of Stained Blood/Bone Marrow Smears and Fixed Cell Suspensions for Complex Molecular Oncology Genotyping – A Practical Specimen Alternative for Molecular Testing in Remote Areas

M Cankovic, S Ali, L Whiteley, D Chitale. Henry Ford Hospital, Detroit, MI.

Background: Molecular oncologic pathology is a highly specialized and emergent field especially in the era of targeted therapy. For reliable molecular results, proper specimen handling to extract high quality nucleic acid is imperative, however; sometimes this may not be possible in remote areas. Here we investigated the feasibility of performing molecular testing on Wright/Giemsa stained (WGS) peripheral blood (PB) and bone marrow aspirate (BMA) smears from overseas and fixed cell suspensions (FCS) left over from cytogenetic testing.

Design: DNA and RNA were extracted from 19 air-dried WGS smears [8 PB, 11 BMA] and from 18 FCS (12 PB; 6 BMA) left over from FISH testing for *BCR/ABL* t(9;22). WGS samples were about 8 weeks old, and had been transported on an airplane for 24 hours to simulate international shipment conditions. DNA and RNA were extracted per standard protocol. DNA/RNA yield and purity were evaluated by spectrophotometry, and integrity by PCR amplification of housekeeping genes (mixture of primer pairs yielding fragment sizes of 100bp, 200bp, 300bp, and 400bp for DNA, and beta 2 microglobulin (B2M), a 120 bp fragment, for RNA/cDNA).

Results: WGS slides: Adequate DNA was isolated from 19/19 samples. While 260/280 OD ratio showed inferior DNA purity and total recovery between 0.15 ug to10 ug, the amplified DNA yielded product sizes of 300 bp for 19/19 samples, and 400 bp for 16/19 samples. RNA from WGS smears was of marginal quality, but low level B2M amplifcation was observed in 15/19 samples. Fixed cells: Adequate DNA was recovered from 17/18 samples. Purity (260/280 OD ratios) ranged from 0.94 to 2.79, with majority being 1.66 to 2.15. Total yield ranged from 0.21 to 61.78 ug. Amplified DNA gave product sizes up to 300 bp for 17/17 samples, and 400 bp for 15/17 samples. Adequate RNA was recovered from 9/18 samples. 7/18 tested positive for *BCR/ABL* t(9;22) translocation, concordant with cytogenetics and fresh sample results. *BCR/ABL* mRNA vs housekeeping gene mRNA copy number ratios were lower in fixed samples than in fresh. All of the *BCR/ABL* positive samples were negative for *JAK2* V617F mutation.

Conclusions: We were able to extract good quality DNA from WGS PB and BMA smears prepared overseas and shipped over long distances, but RNA was of marginal quality and was definitely not suitable for quantitative RNA testing. Qualitative detection of *BCR/ABL* mRNA, can be done on FCS, with sensitivity slightly lower compared to fresh samples.

1923 Validation of a Coamplification at Lower Denaturation Temperature PCR (COLD-PCR) Followed by Sanger Sequencing Method for *KRAS* Mutation Detection in Colon Cancer Specimens

NN Chen, Y El-Gohary, I Ezedi, CN Powers, DS Wilkinson, A Ferreira-Gonzalez, CI Dumur. Virginia Commonwealth University Medical Center, Richmond, VA.

Background: *KRAS* mutations are found in 35% to 45% of patients with colorectal cancer, and it has been shown that tumors harboring wild-type *KRAS* gene are associated with good response to the EGFR targeted therapies. Recently, ASCO and the National Comprehensive Cancer Network (NCCN) have recommended that patients with metastatic (advanced) colorectal cancer should have *KRAS* mutation testing done before treatment decision. However, the heterogeneity of clinical specimens may mask the *KRAS* mutation status, misleading the oncologist in the treatment decision. Here, we employed a novel PCR method combined with direct Sanger sequencing, which resulted in a dramatic improvement of the sensitivity for *KRAS* mutation detection.

Design: Conventional PCR and COLD-PCR followed by Direct Sanger sequencing were used to amplify a 216-bp DNA fragment in exon 2 of the *KRAS* gene from genomic DNA extracted from homozygous and heterozygous cell line mixtures ranging from 10% to 100% mutant DNA, to assess the analytical sensitivity of the method. In addition, 17

formalin fixed paraffin embedded (FFPE) tissue specimens with known *KRAS* mutation status were also tested in a blind experiment. For these samples, *KRAS* mutation status was previously determined in separate laboratories, by direct sequencing and real-time PCR using Scorpions™ technology.

Results: We were able to improve the limit of detection from 25% using conventional PCR to 10% of mutant DNA using COLD-PCR (positive in 95% of the replicate tested) in cell line mixtures. The clinical sensitivity of *KRAS* mutation detection was also increased by the use of COLD-PCR compared to Conventional PCR, as well as by the use of tissue macrodissection as shown in Table 1.

Table 1. Comparison of *KRAS* mutation detection by Conventional PCR and by COLD-PCR

Test Method		Gold Standard		Sensitivity	Specificity
		Mutant	WildType		
Conventional PCR w/ macrodissection	Mutant	11	0	73.33%	100.00%
	WildType	4	2		
COLD-PCR w/o macrodissection	Mutant	14	0	93.33%	100.00%
	WildType	1	2		
COLD-PCR w/ macrodissection	Mutant	15	0	100.00%	100.00%
	WildType	0	2		

Conclusions: COLD-PCR followed by direct Sanger sequencing, combined with macrodissection of the FFPE tissue sections provides a sensitive and economical method for detecting low-level mutant alleles of *KRAS* in clinical samples.

1924 Comparative Analysis of Four Methods of MIB-1 Quantitation in Estrogen Receptor-Positive Primary Breast Carcinomas

MD Darrow, C Chisolm, D Williams, B Chastain, A Page, A Adams, C Cohen. Emory University, Atlanta, GA.

Background: MIB-1, a proliferation marker, is one of the weighted parameters in the twenty-one gene Oncotype Breast Cancer Assay, which quantifies the likelihood of recurrence and assesses the potential benefit of chemotherapy. It is also included in several ASCO and NCCN treatment protocols. Thus, accurate quantitation of the MIB-1 labeling index is essential. The aim of this study is to compare MIB-1 proliferation indices of ER-positive primary breast carcinomas generated by different image cytometric techniques to assess consistency and accuracy of results.

Design: Estrogen receptor-positive primary breast carcinomas from 189 patients with Oncotype DX Recurrence Scores were examined. Using the ACIS III Image Cytometer (Dako), five micron MIB-1 immunostained slides were digitally scanned and assayed for nuclear staining in three 20X "hotspot" fields (recommended by DAKO), and in five, ten (most accurate with the CAS200 image analyzer), and fifteen random 20X fields. Results by these four techniques were compared using the Pearson's correlation coefficient.

Results: When compared to the MIB-1 proliferative indices generated by use of the three 20X "hotspot" field technique recommended by DAKO, the values obtained by the other three techniques all exhibited strong, statistically significant correlation ($p < 0.001$), with correlation coefficients ranging from 0.95 for the 15-field technique to 0.98 for the 5-field technique. In addition, the indices determined by using the random 5-, 10-, and 15-field methods, when compared to each other, showed very strong correlation ($p<0.001$), with correlation coefficients ranging from 0.976 (5-fields vs. 15-fields) to 0.988 (10-fields vs. 15-fields).

Conclusions: In ER-positive primary breast carcinomas, generation of MIB-1 proliferative indices using ACIS III Image Cytometry in three "hotspots", and in five, ten, and fifteen random 20X fields yields very similar results with minimal variation. This finding suggests that, unlike HER2 where quantitation in 10 random fields is optimal, use of any of these four methods in determining MIB-1 values is equivalent and that technique variation in various immunohistochemistry laboratories will not significantly impact resultant MIB-1 indices and subsequent carcinoma stratification.

1925 Touch Imprint Cytology: A Simple Method To Enrich Tumor Cells for Molecular Analysis

S Dogan, J Becker, N Rekhtman, LH Tang, K Nafa, M Ladanyi, D Klimstra. Memorial Sloan-Kettering Cancer Center, New York, NY.

Background: A relative excess of non-neoplastic cells in frozen carcinoma samples is often a cause of false negative results in molecular assays, necessitating painstaking techniques to enrich for tumor cells, such as laser-capture microdissection. Given the lower cohesiveness of epithelial tumor cells compared to non-neoplastic epithelium and mesenchymal stroma, we hypothesized that tumor procurement by touch imprint would provide a simple, cost-effective method to obtain enriched neoplastic cells, compared to frozen whole tumor samples.

Design: Six carcinomas with known *KRAS* mutations were tested: 2 primary colorectal carcinomas (CRCs), 2 liver metastases of CRCs, 1 adenocarcinoma of lung, and 1 adenocarcinoma of pancreas. Two sets of 8 touch imprint slides and 1 frozen whole tumor sample (without major areas of normal tissue), both with a corresponding H&E stained slide, were obtained from each tumor. Stained slides were evaluated by light microscopy to estimate the percentage of carcinoma cells. Extraction of DNA from unstained touch imprints and whole frozen samples was followed by *KRAS* Exon 2 PCR and mutation analysis by direct sequencing. The relative proportion of the mutant allele in a given sample was determined by calculating the height ratio between the mutant and wild type peaks on the sequencing electropherogram. Based on the calculated values we determined the fold increase in the mutant-enriched DNA in touch imprints versus frozen samples.

Results: By light microscopy, touch imprints showed 1.4-3.5 fold (mean 2.1 fold) enrichment in neoplastic cells compared with the frozen tissue. The mutant to wild type peak height ratio was 1.4-7.1 fold (mean 3.3 fold) higher in all 6 touch imprint samples compared with the corresponding frozen sample. The average amount of extracted DNA ranged from 145ng-7ug per touch imprint slide.

Conclusions: Procurement of carcinomas by touch imprint is rapid, simple, and inexpensive, consistently provides a tumor-enriched sample, and is an excellent source of high quality tumor DNA. Touch imprints are a useful method of tumor procurement for molecular analysis, particularly if mutation analysis by direct sequencing is to be performed, as a tumor-enriched sample could compensate for the relatively low sensitivity of direct sequencing.

1926 Immuno-Guided Laser Assisted Microdissection Techniques for Formalin-Fixed Tissue Samples

FC Eberle, JC Hanson, JK Killian, K Ylaya, SM Hewitt, ES Jaffe, MR Emmert-Buck, J Rodriguez-Canales. National Cancer Institute, Bethesda, MD.

Background: Laser assisted microdissection (LAM) has been incorporated in pathology as a tool for molecular profiling. Immuno-guided LAM (I-LAM) is a technique for isolating specific cells after immunohistochemistry (IHC). Current LAM systems incorporate a UV-based cutting laser that requires special membrane slides. For formalin-fixed paraffin embedded (FFPE) specimens the use of membrane slides with standard IHC techniques is not suitable. Moreover, the effects of IHC on both DNA integrity and methylation profile for epigenetic analysis of FFPE specimens are unknown. The goal of this study is to establish an IHC protocol that is compatible with I-LAM of FFPE specimens, and to evaluate the effects of this technique on DNA integrity and methylation profile.

Design: By using 10 FFPE samples (5 primary mediastinal large B-cell lymphoma and 5 classical Hodgkin's lymphoma) we tested different methods of slide preparation, antigen retrieval (AR) and IHC. Tissue sections were either stained with H&E (for LAM) or with anti-CD20 or anti-CD30 (for I-LAM) before tumor cells were microdissected using Leica LMD 6000. DNA was extracted, evaluated for amount and integrity and the global DNA methylation profile of H&E or IHC stained tumor cells of each individual sample was compared using a CpG array platform (Illumina GoldenGate Methylation Array).

Results: The best technique for membrane slide preparation was achieved by UV-irradiation and poly-L-lysine coating. Testing different AR buffers, distinct incubation times and antibody dilutions, we could demonstrate specific target cell staining with high reproducibility in all 10 cases. After following the optimized protocol, tumor cells were isolated by LAM or I-LAM. PCR of extracted DNA from tumor cells showed that DNA integrity was not affected by AR and IHC compared to H&E controls. Global epigenetic profile was not altered by IHC in comparison with H&E showing strong correlation ($r = 0.945$ to 0.981) for CpG target methylation of 1505 analyzed sites.

Conclusions: These results demonstrate the validity and utility of our IHC protocol for I-LAM. IHC does not affect DNA integrity and the epigenetic profile compared to H&E staining. This protocol allows the application of I-LAM for specific genomic and epigenetic analysis from FFPE specimens.

1927 Methodological Improvements Allow the Use of Fractal Geometry as a Prognostic Test in Prostate Cancer

GS Guandalini, V Macias, AK Balla. Armed Forces Institute of Pathology, Washington, DC; University of Illinois at Chicago, Chicago, IL.

Background: Fractal dimension (FD) is a relatively new mathematical concept that quantifies irregularity on a given geometric structure. When applied to anatomic pathology, it measures image roughness or complexity. Several approaches have been reported using this technique on cancer histopathology, but so far fractal geometry has not been successfully used as a prognostic marker. Here we examined some crucial methodological improvements that allowed FD to discriminate recurrence from non-recurrence cases after radical prostatectomy.

Design: The source of tissues was the Cooperative Prostate Cancer Tissue Resource (CPCTR; www.prostatetissues.org). We obtained digital images (800 x 600 pixels) of radical prostatectomy H&E slides from 35 subjects with PSA recurrence, matched for race, age, Gleason grading score and pathology TNM classification with 35 patients without recurrence (n=70); a nested case-control design. All non-recurrence subjects had more than 5-years post-prostatectomy follow-up. Snapshots were taken under 20X, 40X, 100X and 200X to find out the effect of magnification to the overall FD. In a novel approach, we applied digitally automated color, brightness and contrast correction (Microsoft Office Picture Manager). FD was obtained performing the box counting method for different scaling windows (ImageJ, NIH freeware). Wilcoxon signed-rank test was performed to compare the paired groups.

Results: No statistically significant difference was observed for images without color, brightness and contrast correction. Significantly increased difference was observed with increasing image correction steps: With five correction steps applied on 40X images, PSA recurrence cases had lower FD than their non-recurrence matches in 26 of the 35 pairs ($p = 0.004$). Statistically significant results were also observed for 1 and 3 steps corrections at several scaling windows, but only with 40X and 100X magnification.

Conclusions: FD is lower for patients with prostate cancer recurrence when compared to their corresponding disease free matches. This difference suggests that FD might be useful as a prognostic test in prostate cancer; however, enhancing slides color, choosing the proper magnification and using the correct scaling window are decisive procedures to obtain good results.

1928 Digital Slide Diagnosis of Upper GI Biopsies

D Gui, HM Yang, G Gerney, C Magyar, S Hart, S Dry. UCLA, Los Angeles, CA.

Background: Whole slide digital imaging (WSDI) offers an alternative to glass slides for diagnostic interpretation. Prior work has focused on WSDI for frozen section interpretation or second consults. We are not aware of prior studies on use of WSDI for routine GI biopsies. We examined the accuracy and efficiency of WSDI in routine GI biopsies.

Design: Forty-six H&E stained esophageal and stomach biopsies were selected to include diagnoses typical in our GI biopsy service, including: gastric carcinoma (9),

reflux/eosinophilic esophagitis (4), Barrett's esophagus (13), Candida esophagitis (4), and chronic gastritis with (11) and without H. pylori (7). Some slides had more than one diagnosis. Slides were anonymized to ensure pathologists were blinded to the diagnosis. Glass slides were scanned at 20X (Aperio XT). Three pathologists with varying diagnostic experience (current GI fellow, 5 years and 10 years experience) and computer skills reviewed the WSDI, then the glass slides, with 3-14 days between reviews. Final diagnosis, time required, problems encountered, additional stains desired and whether 40X magnification was needed were recorded for all cases.
Results: All WSDI cases of carcinoma, Barrett's esophagus, Candida esophagitis and chronic gastritis without H. pylori were correctly diagnosed by all pathologists. For WSDI H. pylori-associated gastritis, all pathologists requested special stains and/or 40X magnification. Two pathologists were willing to diagnose H. pylori gastritis on WSDI, but with less than 100% confidence. In 50% of cases, all pathologists noted difficulties in distinguishing eosinophils from red blood cells (RBCs) on 20X WSDI. Kappa statistics for final diagnosis was almost perfect to perfect for digital to glass interpretation for each pathologist (0.93 - 1.0). Interobserver agreement for WSDI diagnosis was substantial, ranging from 0.78 - 0.82. On average, WSDI took 2-4 times longer than glass slide interpretation for all pathologists.
Conclusions: Our initial data indicates that gastric carcinomas, chronic gastritis and intestinal metaplasia (Barrett's or gastric) is diagnosed accurately and with confidence on 20X WDSI. Small infectious organisms, such as H. pylori, are difficult to see on 20X. Another unexpected difficulty was distinguishing RBCs from eosinophils at 20X WSDI. Significantly more time was required for digital versus glass slide interpretation, which may diminish with experience (studies in progress). Our study suggests 20X WSDI can be used with confidence for most commonly diagnosed upper GI disorders.

1929 Dissection of the Heart – Ensuring Proper Practice through Portable Video Gross Dissection Demonstration

D Gui, M Fishbein, S Dry. UCLA, Los Angeles, CA.
Background: Pathologists and pathologists-in-training find cardiac dissection to be one of the most challenging gross examinations. In our experience, the heart is most often dissected incorrectly or incompletely. This has serious diagnostic implications. First, gross cardiac pathology often is equally or more critical to the diagnosis than the microscopic findings. Second, the success of cardiac transplantation has resulted in this being a common organ in both surgical and autopsy pathology practice. To ensure our residents learn proper cardiac dissection, we have created an instructional video of a complete heart dissection. This video is described herein and will be demonstrated live at the USCAP meeting.
Design: We used Sony RM-EV100 digital camera (overhead mounted) with high optical zoom, a JVC DVD recorder and an Intel Core 2 Duo Windows platform. Filming was done in the autopsy suite. One pathologist (MCF) wrote the script and performed the live dissection. The audio file was added to the image file with Adobe Premiere. The CD interface is created with Adobe Flash Creative Suite 4. The movie can be saved via Adobe Premiere in a multiple of formats (mov, avi, for mobile devices) to permit maximal flexibility.
Results: The movie is divided in 5 chapters: introduction, basic gross dissection and evaluation of external surface, dissection of coronary arteries, opening the heart, dissection of the AV node and Bundle of His and sampling of the heart for histology. Similar to recreational DVDs, viewers can select a particular chapter for viewing, as well as skip chapters, pause, etc. Approximately 90 minutes of playing time is available. We have provided the movie (avi format) on CDs for residents and pathology assistant students. In addition to the video, the complete audio text is made available as a separate Word file on the same CD. Residents and PA students have enthusiastically accepted this instructional video.
Conclusions: We have successfully created a digital gross instructional video for gross cardiac dissection. Given the enthusiastic response from residents and PA students, we plan to film additional gross video dissections. Additionally, we plan to place the cardiac gross dissection video on our server, accessible from the residents' internal website. We believe these types of videos will play an important role in pathology education, especially for complicated or rare gross dissections. To our knowledge, this is the first digital gross dissection instructional video worldwide.

1930 Immunohistochemistry (IHC) for DNA Mismatch Repair (MMR) Proteins in Colorectal Carcinoma: What Does Scanty Staining for MSH6 Mean?

M Guo, D Klimstra, L Tang, E Vakiani, N Katabi, Z Stadler, M Weiser, J Shia. Memorial Sloan-Kettering Cancer Center, NY.
Background: IHC for MMR proteins is being increasingly used for screening colorectal cancer (CRC) patients for Lynch syndrome as well as for treatment decision making. However, IHC may be affected by various biologic and technical factors, and interpreting staining results remains challenging. Anecdotally, we have observed a scanty staining pattern for MSH6 antibody that could potentially lead to erroneous interpretation. This study aimed at analyzing the frequency and clinical/pathological significance of this aberrant pattern of staining.
Design: IHC stains for MLH1, PMS2, MSH2, and MSH6 of 420 CRC resections from patients fulfilling the revised Bethesda guidelines (age <50; age 50-60 and tumor shows suggestive morphology; or positive personal or family history) were reviewed, and the patterns of MSH6 staining analyzed; 120 tumors were rectal that had neoadjuvant therapy.
Results: Of the 420 cases, 92 had complete loss of staining for MLH1 and/or PMS2 and 32 for MSH2 and/or MSH6. Overall, 9 cases (9/420, 2%) exhibited a scanty staining pattern for MSH6. In these 9 cases, the positively stained tumor cells were often short segments of individual tumor glands (in gland forming tumors), or confined to a limited focus (in poorly differentiated tumors), constituting <10% of the tumor (often <5%). The staining intensity was uniformly strong; and the negatively stained portions of the tumor showed convincing positive internal control. All 9 tumors had normal staining for MSH2, but 5 lost PMS2/MLH1 (n=3) or PMS2 alone (n=2), which constituted 5% (5/92) of all MLH1 and/or PMS2 abnormal cases. One PMS2 negative case was tested for germline mutation and was found to have a pathogenic mutation in *PMS2*, but none in *MLH1*, *MSH2* or *MSH6*. Four of the 9 tumors had normal staining for all other proteins, and all 4 were treated rectal tumors, which constituted 3% (4/120) of all treated rectal tumors tested.
Conclusions: Rare MLH1 and/or PMS2 deficient CRCs as well as post-treatment MMR proficient rectal cancers can show only scanty staining (i.e., near complete loss of staining) for MSH6. Given that *MSH6* contains microsatellites in its coding region, secondary *MSH6* mutation is a likely explanation for this phenomenon in MLH1 and/or PMS2 deficient cancers. In post-treatment cancers, possible explanation includes environmental factors, such as treatment induced hypoxia. Awareness of such a pattern can avoid misinterpretation of IHC results and the consequent unnecessary genetic work-up.

1931 PI3KCA Mutations in Endometrial Cancer. A Comparative Study between Direct Sequencing and a Real-Time Based Technology

J Hernandez-Losa, R Somoza, C Teixido, E Lindo, A Solsona, J Castellvi, A Garcia, H Alazzouzi, S Ramon y Cajal. Vall d´ Hebron University Hospital, Barcelona, Spain; Fundación Institut Recerca Vall d´Hebron University Hospital, Barcelona, Spain.
Background: Alterations in the phosphatidylinositol 3-kinase (PI3K)/AKT signaling pathway are common in endometrial carcinoma. Despite of PTEN status, the gene mutations or amplifications of the catalytic subunit of PI3K (PI3KCA) have been reported. The majority of the mutations map to three sites E542 and E545 in helical domain and H1047 in the kinase domain, and reflect a gain of enzymatic function of the PI3K conferring a proliferative advantage, which act as a dominant oncoprotein. The discordances in the percentage of PI3KCA mutation and the appearance of novel therapies against this pathway justify the incorporation of new methodologies to assess these mutations.
Design: We have compared two different methods for the detection of mutations in the helical and catalytic domains of PI3KCA gene. We used a commercial kit that include a combination of Scorpions and ARMS technologies (PI3K-Mutation Kit, DXS company) versus Bigdye terminator v3.1 Cycle Sequencing Kit in 71 human endometrial cancer samples. The PI3K Mutation Kit detects 4 somatic mutations including in exon 9 (E542K/D E545K) and exon 20 (H1047R). The DNAs were extracted from FFPE tissue samples. We compare the sensitivity of each technology with different dilutions from a positive control PI3KCA gene mutation cell line (HCT116).
Results: The PI3K Mutation Kit detected the H1047R mutation in less than 5% of DNA mutant whereas direct sequencing detected up to 25% of DNA mutant in a background of wild type genomic DNA in cell lines. This high sensitivity was confirmed in human endometrial cancer samples. The Real-time based technology detected a 14% (10/71) of mutants whereas direct sequencing detected only 11% (8/71) in the specific hot spots. On the other hand, the direct sequencing showed different mutations implicating other amino acids such as Q546 (4/71), and E545A (1/71) mutations no detectable by the PI3K Mutation Kit.
Conclusions: The higher sensitivity results obtained with the PI3K Mutation Kit support the use of this technology in different screenings to assess the status of PI3KCA mutations in human endometrial cancer samples. Nevertheless other amino acids substitutions such as Q546, must be evaluated and explore it incorporation in future kits

1932 Automated Brightfield Dual In Situ Hybridization (BDISH) Technique Is Applicable for ASCO/CAP Guideline for HER2 Testing (ISH,IHC) in Breast Cancers: A Comparative Study

T Itoh, H Itoh, A Serizawa, N Kato, S Umemura, RY Osamura. Tokai Uvniersity School of Medicine, Isehara, Kanagaswa, Japan.
Background: In addition to advanced breast cancers(BCs), early BCs have been treated with Trastuzumab and the incidence of HER2 testing has been increased. Heterogeneity of HER2 expression has been recommended to be included in the HER2 report as it is directly related to the therapeutic response(Arch Pathol Lab Med 2009;133:611-612). Our current study is aimed at to elucidate the feasibility of BDISH in interpreting HER2 expression according to ASCO/CAP guideline.
Design: Total 22 cases invasive ductal carcinoma of the breast were subjected to the following HER2 analysis, automated BDISH(Ventana Medical Systems Inc.), HER2/CEP17 Silver ISH(SISH),FISH(Vysis,Abbott). IHC included HercepTest(DAKO), CB11 and 4B5(Ventana Medical Systems Inc.).
Results: By FISH, cases #1-9 showed amplification by ASCO/CAP guideline. #10 and 11 were equivocal being 1,90 and 1.87 respectively. #12-22 were HER2 negative. By SISH, #1-8 and #19(1.18 by FISH)revealed amplification. #11 was equivocal. #10 and other cases were negative. By BDISH, #1-10 showed amplification. #11 and #17(1.30 by FISH) were equivocal. The remaining cases were negative.

Case	ISH			BDISH				IHC		
	FISH	SISH		HER2 Amplification	Report Result			HercepTest	Clone : CB11	Clone : 4B5
		Microscope	VIAS		<1.8 Nega	1.8≤HER2/CH17≤2.2 Equivocal	>2.2 Posi		VIAS	VIAS
1	12.80	3.38		+			■	3+	3+	3+
2	11.02	3.06		+			■	2+	2+	3+
3	10.75	4.88		+			■	3+	3+	3+
4	8.30	3.53		+			■	3+	3+	3+
5	8.18	3.74		+			■	3+	3+	3+
6	6.60	5.15		+			■	3+	3+	3+
7	3.55	4.08		+			■	3+	3+	3+
8	3.38	5.37		+			■	3+	3+	3+
9	3.24	3.78		+			■	3+ (2+)	3+	3+
10	1.90	1.41		+			■	2+	0	0
11	1.87	1.88		Equivocal		1.94		2+	2+	2+
12	1.60	1.23		-	■			2+	1+	1+
13	1.58	1.41		-	1.38			2+	2+	2+
14	1.42	1.24		-	1.32			0	0	0
15	1.33	1.28		-	■			2+	1+	0
16	1.33	1.05		-	1.40			2+	0	0
17	1.30	1.37		Equivocal		1.86		2+	2+	2+
18	1.20	1.21		-	1.43			1+	0	0
19	1.18	2.32		-	■			2+	2+	2+
20	1.18	1.12		-	■			2+	1+	1+
21	1.15	1.58		-	1.47			2+	3+	3+
22	1.07	1.08		-	1.60			1+	0	0

For HER2 IHC, #1-9 were 3+ by 4B5 antibody. Case #2 was 2+ by HercepTest and CB11. #10-13,15-17,19-21 were 2+ by HercepTest. #11,13,17,19,21 were 2+ by CB11. The remaining cases were either 0 or 1+. Thus, 4B5 showed better concordance with ISH.
Conclusions: The combination of BDISH and IHC by 4B5 is expected to serve as good as, or slightly better than, the combination of FISH and HercepTest. Particularly, BDISH is more suitable for the interpretation of heterogeneity of HER2 gene amplification by using light microscope.

1933 Novel Application of SELDI-TOF Mass Spectrometer in Genotyping and Personalized Medicine

M Jin, S Yang, H Wu. Ohio State University, Columbus, OH.
Background: SNPs are genetic markers that determine an individual's susceptibility to various diseases. SNPs have also been used as molecular markers to predict drug efficacy and safety. We postulate that SELDI-TOF mass spectrometer offers an excellent platform for genotyping medically important SNPs for diagnosis and for prediction of therapeutic responses. This hypothesis was tested in several clinical settings, including 1) SNPs influencing warfarin drug sensitivity and safety, 2) SNPs (CYP2D6) predicting patient response to tamoxifen; 3) SNPs (CYP2C19) impacting Plavix's drug efficacy, and 4) SNPs determining genetic risks for clotting disorders.
Design: DNA containing each target SNP was first amplified by PCR using specific primers. Afterwards, single base extension was performed to generate specific SNP product. Finally, genetic variants displaying different masses are bound to Q10 anionic proteinChips and then genotyped using a SELDI-TOF mass spectrometer in a multiplexed fashion.
Results: SELDI-TOF mass spectrometer offers unique properties of on-chip sample enrichment and clean-ups, which streamline the testing procedures and eliminate many tedious experimental steps required by the conventional mass spectrometer based method. The turnaround time by SELDI-TOF mass spectrometer, from sample collection to the report of genotypes for each panel of SNPs, is less than five hours. The analytical accuracy of this method has been confirmed both by bidirectional DNA sequencing and by comparing the genotype results obtained by SELDI-TOF mass spectrometer to reports from a clinical reference laboratory.
Conclusions: By using SELDI-TOF mass spectrometer, we have devised a novel multiplex genotyping method that is fast, accurate, cost effective, and will improve patient care and clinical outcomes through personalized health care.

1934 Mass-Spectrometry-Based Proteinomic Analysis of Amyloid Deposits in Pituitary Prolactinomas

S Kip, B Scheithauer, L Erickson, R Lloyd, A Dogan. Mayo Clinic, Rochester, MN.
Background: Amyloid deposits are rarely seen in pituitary adenomas, mainly prolactinomas. Published data indicate that the amyloid is produced by endocrine rather than mesenchymal cells. Relative to amyloidogenic peptide components of prolactinomas, it has been suggested that amyloid masses contain prolactin.
Design: We report a retrospective study involving 18 prolactinomas associated with amyloid deposits, all operated between 01/1996 and 03/2009, and nearly half being consultation cases.
Results: The study group showed a M:F ratio of 2:1, mean age of both being 46 yrs. Although marked hyperprolactinemia was noted in all, levels were 4x higher in males (2302 ng/mL) than females (552 ng/mL). Respective tumor sizes were 2.82 cm^3 vs. 0.45 cm^3. Of note in 6 cases were spherical, concentric deposits, with radial cracking; 12 lesions featured amorphous intercellular deposits. Both were eosinophilic and, where performed (n=3), Congo Red-positive and birefringent. IHC showed intense Golgi-pattern staining for prolactin (n=12). Ultrastructural analysis revealed 10-13 nm fibrils forming stellate extracellular deposits and grouped in intracytoplasmic bundles (n=2). The amyloid deposits were microdissected from H&E slides and analyzed by mass spectrometry (MS). In all cases, prolactin precursor protein was represented, in conjunction with other known amyloidogenic peptides. Although peptide coverage for prolactin varied slightly among cases, all possible tryptic peptides were identifiable, suggesting that the whole prolactin protein, with the exclusion of most of signal peptide (SP), was the major constituent. Interestingly, last 2 of 28 residues of SP, normally cleaved off, were retained, an observation of unknown physiologic significance. Also, almost all prolactin precursor peptides analyzed showed oxidation of 3 residues at the same location, a finding of unknown significance, perhaps attributable to storage artifact. In one patient, growth hormone precursor was also highly represented, maybe related to high frequency of co-expression of these hormones in a subset of adenomas. Also of note was the presence of structural proteins in small quantities.
Conclusions: Ours is the first in depth, sizeable study of pituitary adenomas showing amyloid deposits in which their protein signature was assessed by MS. The findings indicate that, almost the entire prolactin protein, with the exclusion of most of SP, is deposited by the hormone-secreting tumor cells and comprise the major component of the amyloid.

1935 Microarray Reveals Concomitant Mutations Associated with 5-Fluorouracil Toxicity

DR LaFrance, M Lowery-Nordberg. Louisiana State University Health Sciences Center-Shreveport, Shreveport, LA; Feist-Weiller Cancer Center, Shreveport, LA.
Background: Approximately 30% of patients treated with 5-Fluorouracil (5FU) based chemotherapy develop significant toxic response. Toxicity has been associated with single nucleotide polymorphisms (SNPs) in dihydropyrimidine dehydrogenase (DPYD); thymidylate synthase (TYMS) and methyltetrahydrofolate reductase (MTHFR) have also been implicated. 5FU containing regimens are utilized frequently, however, due to its superior efficacy in the treatment of colon, breast, and head/neck carcinomas. The use of 5FU, along with the recent prioritization of personalized therapy, has highlighted the importance of pre-treatment evaluation of cancer patients for predicting chemotherapeutic response. We propose that the DNA microarray platform can identify SNPs associated with 5FU toxicity, and we predict that patients positive for SNPs will have an increased propensity toward developing toxicity when treated with 5FU.
Design: Using a multiplex microarray detection platform (Infiniti 5FU, AutoGenomics, Inc., Carlsbad, CA), DNA samples from 12 patients were analyzed for specific SNPs. The following were targeted: DPYD (85T>C, IVS14+1G>A, 1590T>C, 1679T>G, and 2846A>T), MTHFR (677C>T and 1298A>C), and TYMS (ins/del TTAAAG in the 3'-untranslated region). For patients with available follow-up information, the development of 5FU related toxicity was compared with mutation status.
Results: DNA microarray technology successfully identified SNPs in 13% of patients tested (4% homozygous, 9% heterozygous). Fifty eight percent of patients identified possessed SNPs in two of the target genes, with 33% having SNPs in *DPYD* and *TYMS*, *MTHFR* and *DPYD* affected in 17%, and 8% with *MTHFR* and *TYMS* SNPs. All 3 genes were affected in 17% of patients tested. Furthermore, 3 out of the 5 patients for which followup information was available demonstrated 5FU related toxicity requiring dose adjustment or treatment discontinuation. Two of the patients developing severe toxicity were positive for mutations in *DPYD* and *TYMS*; the third patient harbored mutations in all three target genes.
Conclusions: DNA microarray technology represents a novel method by which SNPs associated with 5FU toxicity can be detected. Our data supports the position that such mutations may indeed predispose patients to 5FU induced side effects. Additionally, the potential of concomitant mutations to further exacerbate 5FU induced chemotoxicity is intriguing and presents an opportunity for additional research.

1936 Microarray Evaluation of Epidermal Growth Factor Receptor (*EGFR*) Mutation Status

DR LaFrance, M Lowery-Nordberg. LSUHSC-Shreveport, Shreveport, LA; Feist-Weiller Cancer Center, Shreveport, LA.
Background: With the advent of tyrosine kinase inhibitors and the promotion of individualized cancer therapy, stratification of patients with non-small cell lung carcinoma (NSCLC) has moved to the forefront of lung cancer chemotherapy. Molecular studies reveal polysomy for chromosome 7 (location of *EGFR* gene) in many solid tumors, and have implicated the importance of *EGFR* amplification in tumorigenesis. Additionally, the association of *EGFR* amplification with cytogenetic abnormalities in other tumor markers suggests diffuse genomic instability. Interestingly, however, patients with activating *EGFR* mutations have a genetically simpler disease that responds to targeted treatment and has a more favorable clinical outcome. The significance of diagnostic and therapeutic information provided by *EGFR* mutation status as determined by fluorescence in situ hybridization (FISH) has been previously documented by our group (Wei et al. Mod Pathol. 2007; 20(9):905-13). Presently, we will evaluate the DNA microarray platform as a novel method for documenting *EGFR* mutation status in patients with NSCLC.
Design: Unstained slides for 210 cases of NSCLC previously tested for *EGFR* amplification by FISH were collected from LSUHSC-Shreveport pathology archives. DNA was successfully extracted from 70 of these slides using the Pinpoint Slide DNA Isolation System (Zymo Research, Orange, CA). Using a multiplex microarray detection platform (Infiniti, AutoGenomics, Inc., Carlsbad, CA), the isolated DNA was analyzed for *EGFR* mutations in exons 18, 19, 20, and 21.
Results: *EGFR* mutation status was successfully determined by DNA microarray technology. Conclusive data was obtained in 38 of the 70 DNA samples isolated from unstained slides. A subset of the samples tested (11%) were positive for *EGFR* mutations, including two with exon 19 mutations, and two with mutations in exon 20.
Conclusions: The ability to identify which NSCLC patients harbor *EGFR* mutations is key to the strategic planning of oncology treatment. We propose a novel method whereby clinically significant *EGFR* mutations can be identified via a pre-therapeutic screening test. If positive for activating *EGFR* mutations, cancer patients can then be more successfully treated with targeted pharmaceuticals, such as gefitinib and erlotinib. In addition to facilitating the medical goal of individualized cancer therapy, this data may also be used to support preliminary data regarding the utility of biomarkers and other clinical indicators in prognostication and diagnosis of NSCLC.

1937 Comparison of TaqMan PCR and Pyrosequencing Assays for Assessment of KRAS Mutations in FFPE Colorectal Cancer Specimens

JA Lefferts, H Chen, A Suriawinata, GJ Tsongalis. Dartmouth-Hitchcock Medical Center, Dartmouth Medical School, Norris Cotton Cancer Center, Lebanon, NH.

Background: KRAS mutation detection, specifically in the context of colorectal cancer, is being used with increasing frequency due to findings that KRAS mutations predict poor response to certain drugs targeting the EGFR, upstream of KRAS in signaling pathways. Currently, FDA-approved KRAS mutation assays are not available, requiring laboratories wishing to perform this testing to develop their own assays. Here, we evaluate a new method of KRAS mutation detection which uses real-time PCR, producing faster results and eliminating the need for post-PCR manipulation.

Design: Twenty DNA samples extracted from FFPE tissue specimens collected during resection of villous adenomas and adenocarcinomas of the colon were subjected to both pyrosequencing and a TaqMan real-time PCR assay. For pyrosequencing the PyroMark 24 platform was used to sequence codons 12 and 13 following PCR amplification of the region surrounding these codons. In the TaqMan PCR analysis each DNA sample was subjected to a set of seven TaqMan PCR assays, each designed to detect one of seven point mutations in codons 12 and 13 of KRAS.

Results: Twelve of the twenty samples tested were found to have KRAS mutations by at least one of the two assays tested. In one of these samples, both assays gave a G13D signal low enough to make distinguishing it from wild-type samples difficult. The detection of the same mutation by two different assays, however, helped confirm the presence of an actual G13D mutation. Additionally, two separate mutations were detected by pyrosequencing in a sample found to be positive for one mutation by the TaqMan assay; another sample found to contain a G12V mutation by the TaqMan assay failed to amplify in the pyrosequencing PCR, resulting in no pyrosequencing results for this sample.

Conclusions: An initial comparison of KRAS mutation detection assays using real-time TaqMan PCR and pyrosequencing indicates a similar ability of both assays to distinguish between wild-type and mutant genomic DNA with respect to KRAS. Anticipated batch size and laboratory instrumentation available may be among the factors to be considered by laboratories implementing KRAS testing.

1938 A Molecular Touch-Prep Method for Preserving Tumor DNA from Fresh Clinical Specimens

JA Lefferts, ML Petras, A Suriawinata, GJ Tsongalis. Dartmouth-Hitchcock Medical Center, Dartmouth Medical School, Norris Cotton Cancer Center, Lebanon, NH.

Background: Molecular diagnostic laboratories are facing an increasing demand for detecting mutations in tumor samples archived in formalin-fixed, paraffin-embedded (FFPE) tissue blocks. This testing has been driven in part by studies that led the FDA to update anti-EGFR antibody drug labels to mention their lack of benefit in colorectal cancer patients with tumors harboring KRAS codon 12 or 13 mutations. Due to the prevalence of FFPE tumor specimens, DNA isolated from this source is most easily obtained. However, processing of FFPE tissue results in partial fragmentation of DNA and carry-over of PCR inhibitors during extraction protocols. As a potential remedy to this situation, we evaluated the use of Whatman FTA paper cards for collection of fresh colorectal tumor samples before tissue fixation and for isolation of DNA for use in two different KRAS mutation assays.

Design: Eleven colon tumor samples were collected by making a cut into the fresh tumor and applying Whatman FTA paper to the cut surface. The samples were allowed to dry completely at room temperature and held for DNA extraction based on Whatman FTA protocols. KRAS mutation analysis was performed using seven independent custom TaqMan PCR assays (Applied Biosystems). Samples in which KRAS mutations were detected were also subjected to pyrosequencing analysis of KRAS. DNA from matched FFPE tissue blocks from these tumors were also collected for use in the TaqMan analysis.

Results: Of the eleven colon tumors sampled, TaqMan PCR analysis revealed that six were positive for mutations via the Whatman FTA paper preparations. The samples found to have mutations were confirmed by pyrosequencing and by performing the TaqMan PCR testing using DNA isolated from corresponding FFPE tumor specimens. In addition to the six specimens found to have mutations, there were two low-level/equivocal mutations identified via the FTA method which were not identified by pyrosequencing or with the TaqMan assay in DNA isolated from FFPE tissue.

Conclusions: Whatman FTA paper cards provide an intriguing alternative to FFPE tissue for collection of colorectal tumor samples for isolation of DNA and have many advantages including immediate specimen availability, faster DNA isolation protocol, decreased need for hazardous chemicals and potentially higher quality DNA, while still allowing for long-term storage of tumor specimens at room temperature before DNA isolation.

1939 Automated Annotation of Histopathology Data from Final Pathology Reports to Biorepository Samples

E Lickerman, J Sebastian, R Bowman, C Magyar, S Santoro, N Afsheen, A Sharif, S Dry. UCLA, Los Angeles, CA; Daedalus Software Inc., Cambridge, MA.

Background: Rich histopathologic annotation enhances the value of tissue biorepository samples. Unfortunately, no automated, accurate annotation processes exist. Manual data entry underlies most current approaches. To solve this deficiency, we developed an automated procedure that extracts data from standardized sections of the finalized pathology report (PowerPath) and downloads the information to our biorepository database (Biomaterials Tracking and Management Application (BTM™), Daedalus Software Inc.).

Design: Customized synoptic reports (SynR), based on College of American Pathologists recommendations, were developed for each gastrointestinal (GI) system organ. *SynR are imported into the microscopic description section*. Standardized language includes tumor types, grades and staging information. Non-productive text is deleted. Free text is limited to one field. The microscopic section text is imported from PowerPath into BTM. Then, synoptic report text is extracted, parsed and converted into specimen annotations. These annotations are entered into the Lucene text search engine as indices pointing to the surgical pathology case number. Each of these annotations can be used to search for samples from the relevant surgical pathology case.

Results: GI SynR, introduced in 2007, are used routinely by all UCLA GI pathologists. We permit personalized language in the final diagnosis section as SynR in the microscopic description section ensure standardized language. Oncologists and surgeons enthusiastically accepted SynR. Using pancreas as the test case, histopathologic data was imported successfully from the final PowerPath report into BTM and correctly associated with tissue samples. Samples with detailed histopathologic criteria are retrieved easily; for example, mixed acinar-endocrine + uncinate process + pT2. Complex searches using both SynR and other data fields elsewhere in BTM (ie, patient sex, specific research project subjects, etc) also are possible.

Conclusions: Our novel automated process uses SynR to extract standardized histopathology data from final PowerPath reports, then imports and links this data to relevant samples within our BTM biorepository database. Such systematic annotation greatly facilitates biorepository searches and eliminates known problems with free text searching. SynR are customizable by organ. GI pathologists and clinicians have accepted the SynR. Expansion to additional organ systems is being undertaken.

1940 Resolution of HER2 STATUS in Breast Cancer Cases with Equivocal IHC Scores Using a Clinically Validated Array CGH Test for Chromosome 17 Analysis

I Lytvak, SR Gunn, IT Yeh. University of Texas Health Science Center, San Antonio, TX.

Background: Recent multi-probe FISH and array CGH studies have shown that the co-existence of pericentromeric chromosome 17 amplification and HER2 positivity can result in a false negative HER2/cep17 ratio in newly diagnosed breast cancer. This previously unsuspected complexity of chromosome 17 in many breast cancer cases has resulted in a need for the development of alternative methods for resolution of HER2 status. Recent validation of commercially available array CGH tests for analysis of the breast cancer genome provide an alternative high throughput method for accurate determination of HER2 gene copy number and chromosome 17 status. In the current study 20 cases of IHC 2+ invasive ductal carcinoma were analyzed by array CGH for the resolution of HER2 and chromosome 17 status.

Design: Tumor targeted DNA extraction was performed on fresh frozen tumor tissue from 20 cases of invasive ductal carcinoma with IHC scores of 2+. Chromosome 17 analysis was performed using the Her17Scan™ test, a whole genome BAC microarray with 127 probe coverage of chromosome 17 including specific targeting of the pericentormeric region and the *HER2/TOP2A* amplicons.

Results: HER2 gene copy number and chromosome 17 status were resolved in all cases. 18 cases were HER2 negative and 2 cases were HER2 positive by array CGH. HER2 negative cases showed a marked heterogeneity of chromosome 17 structure. The majority displayed a complex pattern of gains and losses of genetic material on both q and p arms, but with no change in the centromeric region.Four cases showed completely normal chromosome 17. One case demonstrated significant gain of genetic material on both arms of chromosome 17 with associated amplification of pericentromeric region. All cases negative for HER2 by array CGH were also HER2 negative by FISH. 2 cases showed amplification of HER2 by array CGH. Complex abnormalities of chromosome 17 were identified including significant gain of genetic material on both arms in one case and multiple gains and losses in another case; no changes in the centromeric region was identified in this group. FISH confirmed HER2 amplification in both these cases.

Conclusions: Array CGH is a robust technique for determination of HER2 and chromosome 17 status in newly diagnosed breast cancer. This test enables evaluation of the entire chromosome 17 thus providing the clinician with additional information that may affect treatment strategies and prognosis.

1941 Multidimensional Shape and Color Distributions as a Computational Biomarker for Cancer Pathology

A Milutinovic, MA Reza, DE Breen, FU Garcia. College of Medicine, Drexel University, Philadelphia, PA; College of Engineering, Drexel University, Philadelphia, PA.

Background: Imaging, both in 2D and 3D, is now a ubiquitous procedure in medicine, science and engineering. The resulting images contain a wealth of information that to date has only been partially utilized. We are developing a computational biomarker for the characterization of breast carcinomas to predict lymph node status.

Design: Our method is based on computational examination of a routinely applied prognostic panel that uses immunohistochemistry and H&E staining of 50 invasive breast cancer carcinomas with known lymph node status. This panel includes: estrogen and progesterone receptors, MIB-1 (proliferative activity), mutated p53 and HER2/neu. The highest staining marker from the panel was selected for further digital image analysis. Using image processing techniques and geometric analysis, the architectural histologic pattern and the expression of these prognostic markers were analyzed to create feature vectors that numerically characterize each tumor's features. Tumor characteristics including pathologic staging were added to the feature vectors. These feature vectors are fed into an algorithm called Support Vector Machines (SVM), which uses a training set of feature vectors to classify unknown samples.

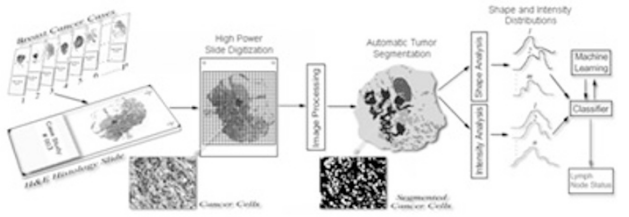

Results: A total of 50 cases were processed to create the feature vectors. Of the 50 cases, 25 were lymph node positive (N1 and higher) and 25 negative (N0). In iterative testing of the algorithm, where one case is used as an unknown specimen and all others are used for training, the best results were obtained using a Radial Basis Function kernel with a sigma parameter of 35. Of the 50 cases, 19 lymph positive and 16 lymph negative cases were correctly classified (0.76 sensitivity and 0.64 specificity).
Conclusions: 1. SVM analysis can predict lymph node status in the majority of patients with invasive mammary carcinoma. 2. Refinement of the feature vector is currently in development to increase specificity and sensitivity. 3. N0 lymph nodes will be further studied using NSABP protocol B-32 to improve specificity in around 11.4% (detection of occult metastases).

1942 Mismatch Repair Protein (MMR) Immunohistochemistry: A 2-Antibody Screening Panel Is Equally Efficacious for Intestinal and Extraintestinal Tumors

A Mojtahed, I Schrijver, JM Ford, TA Longacre, RK Pai. Stanford University Medical Center, Stanford, CA.
Background: Mismatch repair (MMR) protein immunohistochemistry (IHC) is a widely used method for detecting patients at risk for hereditary non-polyposis colorectal carcinoma (HNPCC) syndrome. Recent data suggest a 2-antibody panel approach (PMS2 and MSH6) is an effective screening protocol for colorectal carcinoma, but this has not been independently confirmed and there are limited data concerning this approach for extraintestinal tumors.
Design: 281 cases (219 colorectal carcinoma, 34 skin sebaceous tumors, 22 gynecologic carcinomas, and 6 other extraintestinal tumors) were identified for testing based on concern for HNPCC or pathologic features of MSI. IHC was performed for MLH1, MSH2, MSH6, and PMS2. Protein expression loss was defined as absence of tumor nuclear staining with concurrent positive labeling of normal tissue. MSI PCR was performed on colorectal tumor and normal tissue for microsatellite loci BAT-25, BAT-26, MONO-27, NR-21, and NR-24.
Results: The most common abnormality was concurrent loss of MLH1/PMS2 (38/281, 14%) followed by concurrent loss of MSH2/MSH6 (28/281, 10%). Isolated loss of MSH6 was often seen (11/281, 4%); rare cases demonstrated isolated loss of PMS2 (3/281, 1%). Isolated loss of MLH1 or MSH2 was not observed. For colorectal carcinomas, loss of MLH1/PMS2 and loss of MSH2/MSH6 most often resulted in high MSI (25/26, 96% and 9/12, 75%, respectively).

Table 1. Summary of MMR Results

	Colorectal Neoplasms (n=219)	Skin Neoplasms (n=34)	Gynecologic Neoplasms (n=22)
Immunohistochemical Pattern	No. Cases (%)	No. Cases (%)	No. Cases (%)
Loss of MLH1 and PMS2	27 (12%)	6 (18%)	5 (23%)
Loss of MLH1 alone	0 (0%)	0 (0%)	0 (0%)
Loss of PMS2 alone	3 (1%)	0 (0%)	0 (0%)
Loss of MSH2 and MSH6	12 (6%)	13 (38%)	3 (14%)
Loss of MSH2 alone	0 (0%)	0 (0%)	0 (0%)
Loss of MSH6 alone	6 (3%)	2 (6%)	3 (14%)
Loss of at least 1 protein	48 (22%)	21 (62%)	11 (50%)
All proteins tested intact	171 (78%)	13 (38%)	11 (50%)

6 neoplasms from other extraintestinal sites (CNS, ampulla, stomach) showed intact MMR proteins.
Conclusions: Our findings suggest that a 2-antibody MMR panel with PMS2 and MSH6 may be a sufficient initial screening tool for cutaneous (sebaceous), gynecologic, and colorectal carcinomas. The pattern of MMR protein loss by IHC in extraintestinal sites is similar to intestinal (colorectal) sites.

1943 *In Situ* Hybridization (ISH) for Determination of Fungal rRNA Preservation in Sinonasal Fungal Disease

KT Montone, J Palmer, AC Chiu, DW Kennedy, DC Lanza, VA Livolsi, MD Feldman, I Nachamkin. University of Pennsylvania, Philadelphia, PA.
Background: Sinonasal fungal disease (SNFD) is becoming increasingly recognized and identification of specific pathogens may aid in treatment, particularly those patients with invasive disease. ISH for rRNA has become a means for detecting fungi in tissues. One pitfall of rRNA ISH is not knowing whether the rRNA is preserved following routine tissue processing which in the sinonasal tract may include decalcification or in examples of acute necrotizing invasive fungal rhinosinusitis (ANIFRS) may involve frozen section prior to routine formalin-fixation and paraffin-embedding (FFPE). This study set out to determine the preservation of fungal rRNA sequences in SNFD.
Design: 169 SNFD specimens (15 fungus ball (FB), 96 allergic fungal rhinosinusitis (AFRS), and 58 acute necrotizing fungal sinusitis (ANIFRS)) were studied by ISH using a biotin-labeled locked nucleic acid (LNA) probe targeting pan-fungal rRNA. The 169 tissue specimens included 134 routinely FFPE tissues, 19 that had undergone decalcification followed by FFPE and 16 that had been frozen during intraoperative consultation followed by FFPE.
Results: 124 specimens (73%) were positive for pan-fungal rRNA by ISH. 78% of FFPE specimens were ISH positive while only 42% of decalcified specimens were positive. 12 specimens (75%) which had been frozen prior to FFPE were positive by ISH. ISH was positive in 64% of specimens with positive cultures and 11% with negative cultures. ISH was negative in 23% of specimens with a positive culture. 3% of specimens were negative by culture and ISH although fungal organisms were seen by histology. Based on histopathology, ISH was positive in 79% AFRS, 80% FB and 62% of AFIRS.

Diagnosis		ISH Positive		
	FFPE	DCAL	FS	Total
FB	9/12 (75%)	3/3 (100%)	0	12/15 (80%)
AFRS	73/84 (87%)	3/12 (25%)	0	76/96 (79%)
AFIRS	22/38 (58%)	2/4 (50%)	12/16 (75%)	36/58 (62%)

Conclusions: Most SNFD specimens have preserved fungal rRNA with preservation being greatest in non-invasive cases. Decalcification of sinonasal specimens may limit rRNA preservation in SNFD limiting ISH. In routine FFPE, preservation of rRNA is lowest in ANIFRS possibly due to the extensive necrosis encountered in these tissues which may relate to organism viability. Of note, >30% of ANFIRS patients showed no growth in cultures. Intraoperative consultation via frozen section allows for preservation of fungal rRNA in the tissues. Pathologists should be aware that there may be some limitations of using rRNA ISH in SNFD.

1944 The Value of Laser Scatter Microscopy in Clinical Cytometry

EK Morgen, WR Geddie. University Health Network, Toronto, ON, Canada; University of Toronto, Toronto, ON, Canada.
Background: Flow cytometry has traditionally lacked the ability to assess the morphology of analyzed cells. In recent years, this has been addressed by quantitative imaging cytometry (QIC), a slide-based method, and by certain flow cytometers, such as the Amnis ImageStream. The advantage of the latest generation of QIC for cell-surface-marker immunophenotyping lies in its lower cell-number requirements, ability to iteratively re-stain samples, and the high-quality images produced by laser scatter microscopy (LSM), a differential-interference-contrast-like modality. Furthermore, it captures a complete data set for the entire slide, instead of only when certain predefined criteria indicate that an "event" has occurred. Evaluation of cell morphology in cytometry is an important idea, yet the usefullness of LSM in triage and immunophenotyping remains relatively unexplored.
Design: 50 consecutive cases requiring immunophenotyping were analyzed on the CompuCyte iCys, a 2nd-generation quantitative imaging cytometer. The machine generates a series of scan fields, each 748 by 1000 pixels, by directing the microscope stage to move in the x-direction and the laser beam to scan back and forth in the y-direction. For each pixel, the iCys records laser scatter (detected with a laterally-offset photodetector that yields LSM images), light loss, and multiparametric fluorescence data. In each case, LSM was used both for initial cytology specimen triage and as an adjunct to immunophenotyping, and its utility in these roles was evaluated.
Results: LSM produced shaded relief images which clearly distinguished cells from each other, enabled assessment of cell and nuclear contours, and could provide details of chromatin pattern and cytoplasmic features. During triage, these images allowed for sufficient pattern recognition to provide a provisional diagnosis, and thus better selection of antibody panels for immunophenotyping or more appropriate ancillary studies (cell block, molecular, etc.). As an adjunct to immunophenotyping, LSM images were helpful in confirming cell lineage in gating, in excluding granulocytes from a gate (they can exhibit nonspecific fluorescence), and in excluding cell doublets or aggregates from a gate.
Conclusions: Laser scatter microscopy in quantitative imaging cytometry adds high-quality morphologic data that is useful during triage and immunophenotyping in clinical cytopathology.

1945 Time and Temperature Stability of T-Cell Subsets

H Olteanu, CB Schur, AM Harrington, SH Kroft. MCW, Milwaukee, WI.
Background: Enumeration of T-cell subsets in HIV patients (pts) is routinely performed for monitoring infection stage, and for estimating the efficacy of antiretroviral therapy. The gating strategy and the methodology (single vs. dual platform) can have significant impact on results. Studies have examined the effect of specimen refrigeration and age for single-platform (SP) methods, but there is only limited data for time and temperature requirements of dual-platform (DP) methods.
Design: Peripheral blood (PB) from 52 HIV pts was analyzed at room temperature (RT) at 24, 72, and 96 hours. Also, PBs from 34 HIV pts had baseline RT analysis within 24 hours, and then were stored at 4°C and analyzed at 24, 48, and 72 hours. We used a DP method with a CD3/CD8/CD45/CD4 cocktail and a CD45/SSC primary gate (FSC/SSC secondary gate). CBC data were determined at baseline. The coefficient of variation (CV) and residuals (changes in lymphocyte subsets) were recorded at each time point and compared to assess the precision and bias under the various conditions. Linear regression was used to compare the testing performance under different conditions.
Results: The median white blood cell and absolute lymphocyte counts were: 4,950/ul and 1,895/ul (all), 4,000/ul and 1,560/ul (CD4≤300/ul), 5,200/ul and 2,150/ul (CD4>300/ul). Results are summarized in tables 1 and 2. Median residuals were <30/ul for absolute CD4 and CD8 determinations.

table 1

Protocol precision at RT (mean %CV)					
T cells	n	CD4 abs	CD8 abs	CD4%	CD8%
All	52	6.3	2.5	6.4	2.0
CD4≤300	20	7.3	2.4	7.3	1.8
CD4>300	32	5.6	2.6	5.8	2.2
Protocol precision at 4°C (mean %CV)					
T cells	n	CD4 abs	CD8 abs	CD4%	CD8%
All	34	4.6	2.6	3.5	1.9
CD4≤300	12	5.8	3.0	4.8	2.1
CD4>300	22	3.9	2.4	2.9	1.8

table 2

Linear regression analysis for protocol correlation			
x-axis	y-axis	r2	slope
CD4 abs			
24 hrs RT	72 hrs RT	0.9896	1.0360
24 hrs RT	96 hrs RT	0.9746	1.0902
CD8 abs			
24 hrs RT	72 hrs RT	0.9898	0.9750
24 hrs RT	96 hrs RT	0.9870	0.9983
CD4 abs			
24 hrs RT	24 hrs 4°C	0.9971	0.9499
24 hrs RT	48 hrs 4°C	0.9954	0.9395
24 hrs RT	72 hrs RT	0.9907	0.9169
CD8 abs			
24 hrs RT	24 hrs 4°C	0.9962	1.011
24 hrs RT	48 hrs 4°C	0.9940	1.032
24 hrs RT	72 hrs RT	0.9923	1.042

Conclusions: Our results are similar to those published for SP methods for aging or refrigerated specimens. The high level of agreement between measurements performed under different conditions supports the robustness of this DP methodology.

1946 PAX-8 as a Marker for Renal, Müllerian, and Thyroid Differentiation. A Comprehensive Study

A Ozcan, Y Ge, M Rust, G Hamilton, B Krishnan, LD Truong. The Methodist Hospital, Houston, TX; Baylor College of Medicine, Houston, TX; Gulhane Military Medical Academy and School of Medicine, Ankara, Turkey.

Background: PAX-8 is a transcription factor that is essential in embryonic development of kidney, Müllerian organs, and thyroid . PAX-8 may also play role in tumor development in these organs. The diagnostic utility of PAX-8 has not been comprehensively studied.

Design: Formalin-fixed, paraffin-embedded tissue samples for non-neoplastic tissue (n=523 cases), primary neoplasms (n=498), and metastatic neoplasms (n=248) were subjected to immunostain for PAX-8.

Results: Non-neoplastic tissue: PAX-8 was *constantly* noted in glomerular parietal epithelial cells, renal collecting ductal cells; atrophic renal tubular epithelial cells regardless of nephronic segments; epithelial cells of endocervix, endometrium, and fallopian tube, seminal vesicle, epidydimis, and thyroid; and lymphoid cells. PAX-8 was not seen in the rest of tissue samples. **Primary neoplasms**: PAX-8 was expressed by 118/122 renal cell carcinomas (RCCs), 21/21 renal neoplasms other than RCC or transitional cell carcinoma, 132/139 Müllerian-type of neoplasms of ovary or endometrium, 20/20 thyroid follicular cell neoplasms, and 12/12 nephrogenic adenomas. PAX-8 was not seen in other neoplasms. **Metastatic neoplasms**: PAX-8 was expressed by 116/130 metastatic RCCs; 24/25 metastatic Müllerian tumors, and 3/3 metastatic thyroid follicular neoplasm. PAX-8 was not seen in other metastatic neoplasms. The staining was nuclear. Regardless of the diagnosis, the vast majority of cells were stained in the positive cases.

Conclusions: Routinely processed tissue is eminently suitable for optimal PAX-8 immunostain. PAX-8 is a very sensitive marker for non-neoplastic tissue, primary neoplasms, and metastatic neoplasms of renal, Müllerian, and thyroid origin.

1947 A New Approach to Evaluating the Sub-Areolar Margin in Nipple-Sparing Mastectomies: Touch Preparation v. Frozen Section Analysis

NM Patel, L Liu, RA Goldschmidt. NorthShore University HealthSystem, Evanston, IL.

Background: Nipple-sparing mastectomy (NSM) is an alternative to traditional mastectomy for patients undergoing surgery for the treatment and/or prophylaxis of breast cancer. Since the nipple-areolar complex may be involved by pathological processes, intra-operative frozen section analysis of the sub-areolar margin (SAM) is performed at our institution. This method of analysis is often time consuming due to the difficulty of cutting fatty breast tissue and the occasional necessity of multiple chucks and levels, but has a concordance of 100% with permanent section diagnosis at our institution (n=104). Intraoperative cytologic evaluation of the SAM through touch preparation (TP) is an alternative method that has not previously been examined in depth.

Design: TP of the SAM from NSM specimens were made prior to traditional frozen section analysis. All slides were then evaluated for the presence of epithelial and mesenchymal cells and benign and malignant processes. The TP and frozen section slides were then independently compared to those from permanent section to evaluate for diagnosis concordance. Preparation times for single specimen TP versus single specimen frozen sections were also calculated.

Results: Concordance of TP, frozen section, and permanent section diagnoses was 100%(n=11). Benign ductal epithelial cells were seen on all TP. Benign apocrine metaplasia was seen in 2 TP from 2 SAM with fibrocystic change. Significant amounts of mature adipose tissue were seen in 2 TP from 2 SAM with greater than 70% adipose tissue. No carcinoma or carcinoma-in-situ was identified. The average and median time to prepare TP was 4 minutes (range 3-5), as opposed to an average of 10.7 minutes and a median of 9 minutes (range 3-31, n=33) for frozen sections.

Conclusions: Our data suggests that cytologic evaluation of the SAM is a viable alternative to frozen section analysis. In addition, single specimen preparation times for TP are shorter and have less variability than those for frozen sections. We are evaluating additional SAM through TP to further characterize its diagnostic value, since a small percentage (4.5%) of patients undergoing NSM at our institution have had positive SAM.

1948 The Value of PAX-2 for the Work-Up of Metastatic Carcinoma of Unknown Primary: An Immunohistochemical Tissue Microarray Study of 694 Cases

TC Pereira, SM Share, AV Magalhaes, JF Silverman. Allegheny General Hospital, Pittsburgh, PA; Universidade de Brasilia, Brasilia.

Background: PAX2 is a transcription factor that acts to regulate the expression of genes involved in mediating cell proliferation and growth, resistance to apoptosis, and cell migration. By employing tissue microarray technology, we evaluated the expression of Pax-2 in 694 carcinomas from various sites in order to determine its' utility in the work-up of metastatic carcinoma of unknown primary.

Design: IHC was performed for Pax-2 on paraffin embedded sections from tissue microarray of 694 cases of carcinomas from different organs. Cases were interpreted as positive if at least 5% of tumor cells had nuclear staining.

Results: The results of positive cases per primary site are listed as percentage of positive cases % (Number of positive cases/Total number): Lung 0% (0/113), renal cell carcinoma 65.38% (34/52), GI endocrine/neuroendocrine carcinoma 0% (0/20), stomach adenocarcinoma 0% (0/14), esophageal adenocarcinoma 0% (0/20), pancreas carcinoma 4.44% (2/45), prostate carcinoma 0% (0/38), urothelial carcinoma 2.82% (2/71), hepatocellular carcinoma 0% (0/12), cholangiocarcinoma 11.11% (1/9), colorectal carcinoma 0% (0/67), salivary gland carcinoma 6.67% (1/15), breast carcinoma 6.25% (5/80), thyroid carcinoma 8.89% (4/45), endometrium carcinoma 46.15% (18/39), cervix carcinoma 0% (0/11), ovary carcinoma 8.6% (8/43).

Conclusions: Pax-2 is mostly expressed in renal cell carcinoma (65.38%) and endometrial carcinoma (46.15%), with limited to absent expression in carcinomas of other primary sites. We believe that Pax-2 is a useful marker for the work-up of metastatic carcinoma of unknown primary site, especially if renal cell or endometrial carcinoma is considered in the differential diagnosis.

1949 Can We Tell the Site of Origin of Metastatic Squamous Cell Carcinoma? An Immunohistochemical Tissue Microarray Study of 194 Cases

SM Share, TC Pereira, EP Conroy, AV Magalhaes, JF Silverman. Allegheny General Hospital, Pittsburgh, PA; Universidade de Brasilia, Brasilia, Brazil.

Background: In the work-up of metastatic squamous cell carcinoma (SCC), commonly used immunohistochemical (IHC) markers such as K903, p63, and CK5/6 help to confirm a squamous malignancy, but the IHC stains do not determine the primary site of origin. Moreover, unlike adenocarcinoma, IHC has not been well studied in the work-up of metastatic SCC of unknown primary. We compared the specificity of commonly used IHC markers known to support specific tissue sites, including TTF-1, CK 7, CK 20, Villin, p16, and CDX-2, to the commonly used squamous IHC markers, K903, CK 5/6, and p63.

Design: Using a tissue microarray, we compared 194 SCC cases from the following sites as follows: 35 lung, 34 skin, 14 cervix, 4 vagina, 16 vulva, 8 penis, 9 anus, 3 rectum, 10 esophagus, 4 bladder/urethra, and 57 head and neck (4 eye/orbit, 2 parotid gland, 19 tongue, 10 tonsil, 5 oral cavity, 4 pharynx, and 13 larynx). All IHC stains were interpreted to be positive if 5% or more of the malignant cells were positive, regardless of the staining intensity.

Results: p63, and K903 stained positively in 100% of cases, and CK 5/6 in nearly 100% of cases of SCC, with the exception of 2 lung SCC. TTF-1 staining was seen only in 2 of 35 lung SCC, and was negative in all other sites. Positive staining for CK 7 ranged from 12.5% in esophagus and anus to 100% in vagina. CK 20 was positive in 3.1% of lung SCC, and was negative in all other sites. CDX-2 was positive in 7.1% of vulva SCC, and was negative in all other sites. Positive staining for p16 ranged from 21.4% in vulva SCC to 75% in vagina and anus, and was negative in lung, penis, bladder/urethra, and head and neck sites other than the oral cavity. Villin was negative in all cases.

Conclusions: Although commonly used SCC markers are very sensitive and specific, they do not help identify the primary site of tumor origin. TTF-1 showed marked specificity for lung SCC, but had very low sensitivity. P16 showed high sensitivity for GYN, anal, and oral cavity primaries, but exhibited low specificity. CDX-2 was found to be positive only in some vulvar SCC, and CK 7 was negative in SCC from the penis and oral cavity. We conclude that the primary site of SCC cannot confidently be determined by IHC alone, but certain site specific IHC markers can help in identifying the primary site in occasional cases.

1950 Sensitivity of In-Situ Hybridization (ISH) for High-Risk Human Papillomavirus (HR-HPV) in Head & Neck Squamous Cell Carcinoma (HNSCC)

TM Stevens, ST Dunn, S Caughron, Z Gatalica. Creighton University, Omaha, NE; The University of Oklahoma Health Sciences Center, Oklahoma City, OK; Yellowstone Pathology Institute, Billings, MT.

Background: High risk HPV has been implicated in the etiology of a subset of HNSCC, particularly oropharyngeal squamous cell carcinomas. It has also been reported that HPV-related HNSCC carry a more favorable prognosis and are more radiosensitive than their HPV-negative HNSCC counterparts. HR-HPV has been detected in 20-90% of HNSCC, but is generally found at lower transcript levels than in cervical squamous cell carcinomas. Accordingly, a highly sensitive and specific assay for HPV detection is necessary. ISH for HR-HPV allows for direct visualization of HPV integration, thus circumventing the contamination problems inherent in other molecular assays. The sensitivity of ISH remains untested in HNSCC, however.

Design: In this study, 101 HNSCC were tested for high risk HPV by in-situ hybridization method (ISH iView™ Blue Plus, Ventana, Tucson, AZ, performed at Creighton Medical Laboratories) and results compared to PCR (YPI) and Linear Array® (Roche Diagnostics, Branchburg, NJ, performed at University of Oklahoma).

Results: ISH for HR-HPV had sensitivities of 74 and 59%, when compared to PCR and Linear array, respectively (McNemar's test P>0.05 and <0.05 for PCR and Linear array,

respectively). The negative predictive value of ISH for HR-HPV was 80% and 61%, as compared to PCR and Linear array methods, respectively. The specificity of ISH for detection of HR-HPV in HNSCC was 85% and 86%, respectively, when compared with PCR and Linear array. Tumor necrosis and the presence of bacterial contamination were identified as potential sources of false-positive ISHs. HR-HPV was detected in 53, 43, and 39% of HNSCC by Linear array, PCR, and ISH, respectively.
Conclusions: Compared to PCR and Linear array detection methods, ISH for HR-HPV in HNSCC shows good specificity. When compared against both PCR and Linear array as "gold" standards, ISH for HR-HPV in HNSCC has a relatively low NPV and low sensitivity, suggesting possibly that the more sensitive PCR and Linear array methods are more likely to detect clinically irrelevant "bystander" HPV DNA in HNSCC. In summary, ISH for HR-HPV is a highly specific test and allows for direct visualization of integrated HPV DNA thus allowing confident detection of biologically relevant HPV infection in HNSCC. In this series, the percentage of HNSCC harboring HR-HPV DNA is similar to previous reports.

1951 Detection of Giardia Lamblia by Sytox® Green Nucleic Acid Stain in Duodenal Biopsies

BJ Swanson, LL Prestridge, AJ Lazenby. University of Nebraska Medical Center, Omaha, NE; Boys Town National Research Hospital, Omaha, NE.
Background: Giardia Lamblia is the most common gastrointestinal parasite to infect humans. Light microscopic detection of Giardiasis is often difficult because the organisms are indistinct and maybe confused with mucous and blebs of cytoplasm. Recently, CD117 was described as staining the nuclei of Giardia (Sinelnikov et al., 2009). Sytox Green nucleic acid stain has been described as localizing Giardia in stool specimens, but not in tissue. The aim of this study was to determine if Sytox Green nucleic acid stain could detect G. lambia in paraffin embedded duodenal biopsies and compare this to CD117 immunostaining.
Design: Archived paraffin blocks of duodenal biopsies (n = 6) from giardiasis diagnosed by light microscopy were recut at 4 microns. After deparaffinization and rehydration, cases were incubated with Sytox Green nucleic acid stain for 10 minutes, then visualized under a fluorescent microscope. CD117 immunostaining was performed using the antibody from Cell Marque, clone YR145.
Results: G. Lamblia were readily visible by Sytox Green nucleic acid staining in all six cases examined. Furthermore, G. lamblia could be visualized at 20X in all cases. However, CD117 was negative in all six cases by CD117 immunostaining. Internal controls (mast cells) were positive on the CD117 immunostained slides.

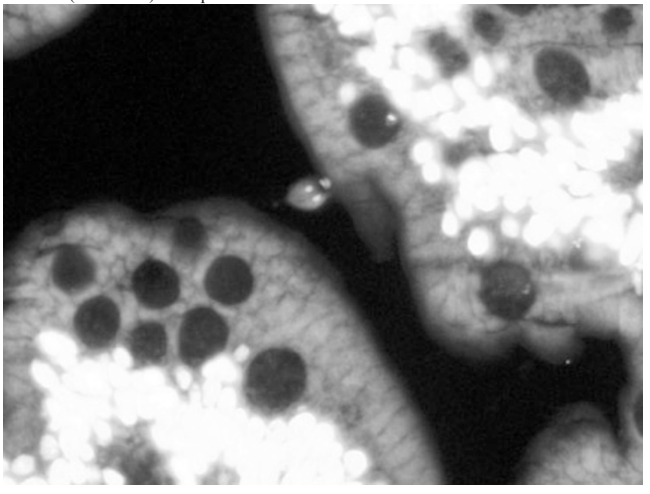

Conclusions: Sytox Green nucleic acid stain reliably detected G. lamblia. While immunofluorescence is routinely used in stool specimens, this is a novel application for immunofluorescence to be used in formalin-fixed paraffin-embedded tissues. Sytox Green stain is a simple, one step process consisting of one incubation with one reagent. Furthermore, staining is rapid and relatively inexpensive. Giardia lamblia did not stain positive with our CD117 antibody. It should be noted that our antibody is from Cell Marque whereas Sinelnikov et al. utilized an antibody from DAKO. In summary, Sytox green stain may be useful in duodenal biopsy cases where giardiasis is suspected but not definitive.

1952 Spiral Tissue Microarray Covers Tissue Heterogeneity of Pulmonary Adenocarcinoma

S Tominaga, R Ohsawa, T Tanaka, S Shimizu, T Hori, J Fukuoka. Toyama University Hospital, Toyama, Japan.
Background: We have recently developed a novel tissue microarray (TMA) technique named Spiral TMA (S-TMA). S-TMA block can be constructed not by coring the tissue from donor block but by embedding multiple reeled thick-cut specimens vertically to a designed recipient block. Its two biggest advantages are that it is applicable to the block with limited tissue and skip damaging donor blocks by coring. It is also assumed that it may cover tissue heterogeneity more than conventional TMA (c-TMA). Lung cancer is one of the tumor with vast tissue heterogeneity where commonest histological subtype is a mixed subtype. Tissue heterogeneity likely reflects difference of molecular biology in each subtype, and for the molecular expression analysis, it is not a negligible factor. To examine if S-TMA covers tissue heterogeneity more than c-TMA, we immunohistochemically investigated the degree of heterogeneity covered by each TMA.
Design: Recent 25 pulmonary adenocarcinoma cases were selected from archives of Toyama University Hospital. S-TMA was constructed with 100 micron thick sections of the blocks. c-TMA with 2mm cores was also constructed. MIB-1, EGFR and CK7, known to have tissue heterogeneity with various degrees were selected. MIB-1 index was scored in areas with both highest and lowest percentage at HPF. For EGFR and CK7, Intensity Score (IS) was divided into 4 degree; 0,none; 1,weak; 2,moderate; 3,strong. Areas with both strongest and weakest IS were scored for EGFR and CK7. The heterogeneity was evaluated by the subtraction between those two scores. Student *t* test and Mann-Whitney's U test was used for the statistical analysis.
Results: Areas seen in S-TMA ranged from 1.0 to 2.04mm^2 (mean 1.44mm^2), while those in c-TMA were always 3.14mm^2. Six cases in c-TMA showed < 1% of MIB-1 index while 3 cases in S-TMA showed < 1% of index. In EGFR and CK7, c-TMA showed 7 and 1 negative cases, respectively, while S-TMA showed 8 and 0. The range of MIB-1 index was significantly larger in S-TMA than in c-TMA. ($p=0.04$). The range of IS was also significantly larger in S-TMA than c-TMA in both EGFR and CK7 ($p < 0.01$).
Conclusions: Our results indicate that Spiral TMA covered tissue heterogeneity significantly more than conventional TMA which was confirmed by expressions of MIB-1, EGFR and CK7, even with smaller areas than conventional TMA included in the array slides. S-TMA may be a useful tool to examine biomarkers in disorders with high tissue heterogeneity.

1953 DNA Quantity and Quality from Paraffin Blocks: A Comparison of Fixation, Processing and Nucleic Acid Extraction Techniques

G Turashvili, M Carrier, N Gale, Y Ng, K Chow, L Bell, M Luk, S Kalloger, B Gilks, S Aparicio, D Huntsman. BC Cancer Agency, Provincial Health Services Authority, Vancouver, BC, Canada; Vancouver General Hospital, University of British Columbia, Canada, BC, Canada.
Background: DNA extracted from paraffin blocks can be used for mutation detection, copy number analysis and most recently whole genome or exome sequencing using Next Generation Sequencing. Although the capacity to extract high quality DNA from paraffin blocks is of more importance now than ever, there is little information available to guide laboratories in their selection of tissue fixation, processing and DNA extraction techniques.
Design: Nine samples (three each of colon, liver and muscle) were subjected to the following fixation and processing conditions: 1. frozen; 2. neutral buffered formalin (NBF) fixation <24 hours; 3. NBF fixation 7 days; 4. molecular fixative (MF) <24 hours; 5. MF 7 days. NBF-fixed samples were processed by standard processing (Tissue-Tek VIP5 processor, Somagen, Canada), and MF-fixed samples by rapid processing (Tissue-Tek Xpress, Somagen). DNA was extracted using phenol-chloroform manual extraction, RecoverAll (Ambion, USA), Waxfree DNA (Trimgen, USA), and QIAamp DNA FFPE Tissue Kit (Qiagen, Canada). DNA quantity and quality were assessed using Nanodrop, and PCR was attempted for amplicons of five lengths (268-1300 bp).
Results: Manual extraction yielded the highest amount of DNA followed by Waxfree DNA, QIAamp and finally RecoverAll kit, independent of the type of tissue, fixation or processing. For all five amplicons used, there were no significant differences between MF-fixed and frozen tissues, and between manual and Waxfree DNA kits on PCR. High molecular weight (1300 bp) DNA was preserved in MF-fixed tissues stored for <24 hours or 7 days, with no difference among the four kits ($p>0.05$). For NBF-fixed tissues, all kits performed similarly except for RecoverAll kit and manual extraction which amplified 536-989 bp and 536 bp fragments, respectively, in fewer samples than other kits ($p<0.02$). Short DNA fragments (268 bp) were successfully amplified in all tissue types using all kits.
Conclusions: The molecular fixative regardless of the duration of fixation, and the rapid processing system used in this study were able to preserve large DNA fragments in paraffin blocks, making these techniques suitable for use in molecular assays, particularly those involving sequencing technologies.

1954 Flow Cytometric Analysis of Ep-CAM Expression Is a Useful Adjunct in the Detection of Metastatic Carcinoma in Fine Needle Aspirates and Body Fluids

L Vila, P Boonsakan, Y Li, RC Braylan, SZ Al-Quran. Univ. of Florida, Gainesville, FL.
Background: Few studies have shown that flow cytometric (FCM) analysis can be used in the identification of non-hematopoietic malignancies. Ber-EP4 monoclonal antibody (AB) is directed against Ep-CAM glycoproteins expressed on virtually all epithelial cells, but is lacking on non-epithelial cells including mesothelial cells. It has been used to differentiate adenocarcinomas from reactive and neoplastic mesothelial cells. The aim of our study was to evaluate the utility of FCM analysis of Ep-CAM expression in the detection of metastatic carcinoma in fine needle aspirates (FNAs) and body fluids (BFs).
Design: We searched for FNAs and BFs received in our laboratory between 2008-2009 that had FCM with Ber-EP4 AB. In all cases, concurrent cytology, including cell block when available, was separately reviewed by cytopathologists. Neoplastic epithelial cells were initially identified by combined analysis of light scatter and CD45 (large CD45-negative cells), and subsequently confirmed by staining with Ber-EP4 FITC AB. Other informative antigens (CD56, CD38, CD117, CD15) were analyzed when cells were available.

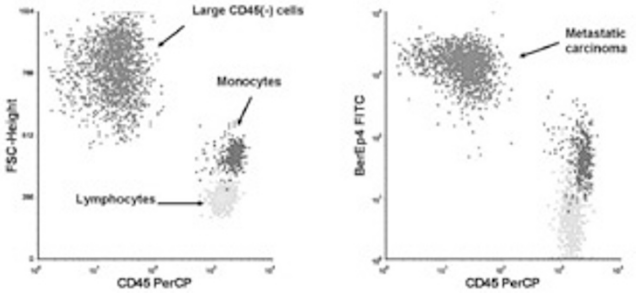

Results: We studied 30 cases including: 18 FNAs (11 lymph nodes, 2 mediastinal, 1 submandibular, 1 lung, 1 pancreas, and 2 liver masses) and 12 BFs (6 pleural, 1 peritoneal, 1 pericardial, and 4 CSF). Metastatic carcinoma was identified in 25 cases by Ber-EP4 positivity. In one case, large CD45- and CD56+ cells, consistent with metastatic carcinoma, were identified by FCM but were Ber-EP4-. Concurrent cytology diagnoses were as follows: positive in 10 cases (confirmed by biopsy in 2 cases), indeterminate/suspicious in 7 cases (confirmed by biopsy in 4 cases), and negative in 4 cases (biopsy and/or repeat cytology showed metastatic carcinoma in all). Five cases did not have concurrent cytology, but malignant cells were identified in our cytospin preparation. Four cases were negative both by FCM/Ber-EP4 and cytology.
Conclusions: FCM analysis of Ep-CAM expression with Ber-EP4 AB can serve as a useful adjunct to diagnostic cytopathology, and in some cases may be superior to morphologic examination, in detection of metastatic carcinoma in small FNA samples and body fluids.

1955 A Simple and Very Flexible Top Pin Tissue Arrayer Using Loose Pins

UF Vogel. University Hospital, Eberhard-Karls-University, Tuebingen, Baden-Wuerttemberg, Germany.
Background: Paraffin tissue microarrays (PTMAs) are constructed by injecting paraffin tissue core biopsies (PTCBs) into preformed holes of a recipient block. These holes can be punched (Kononen), drilled (Vogel) or poured (Mengel). Devices to pour the holes normally consist of a modified steel mold with steel pins at the bottom (Figure 1A; TMA builder, LabVision). So, the size of the recipient block and the arrangement and the number of the holes are determined by the steel mold. To make the system more flexible I designed a device which uses ordinary steel molds of different size, a spacer plate with loose steel pins and a perforated plate. In contrast to the modified steel molds the steel pins are placed from above into the ordinary steel molds and are loose.
Design: 375 holes (diameter: 1.05 mm; distance of the holes: 0.3 mm) were drilled into a spacer plate (POM-C; Figure 1 B,C; S spacer plate) and a perforated plate (nickel silver; Figure 1B,C; P perforated plate) within an area of 32 x 20 mm². Depending on the desired number of holes in the future PTMA up to 375 steel pins (diameter: 1.0 mm; length: 30 mm) were put into the holes of the spacer plate. The steel pins had a 1.2 mm swelling at one end to prevent gliding through the holes. The spacer plate equipped with the desired number and arrangement of steel pins, the perforated plate, a plastic cassette (Figure 1C; C cassette) and an ordinary steel mold (tissue-tek; Figure 1C; M mold) were put together like a sandwich and filled with liquid paraffin. Optionally, a cover plate (Figure 1BC; CP cover plate) was added to prevent the loose steel pins to fall out of the spacer plate. After solidification, the sandwich was disassembled to release the recipient block (Figure 1D). Paraffin tissue core biopsies were manually injected into the holes of the recipient block. The PTMAs were cut and the sections were stained according to routine procedures.

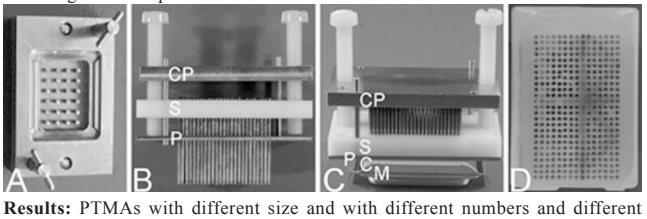

Results: PTMAs with different size and with different numbers and different arrangements of the PTCBs were successfully constructed.
Conclusions: With the novel device consisting of a spacer plate, a perforated plate and loose steel pins it is possible to pour recipient blocks using ordinary steel molds of different size making the system very flexible.

1956 Adipophilin Expression in Lipomatous Tumors and Undifferentiated Pleomorphic Sarcomas

W-L Wang, MT Deavers, VG Prieto, AJ Lazar, D Ivan. UT-M.D. Anderson Cancer Center, Houston, TX.
Background: Adiopophilin is a membrane associated protein surrounding intracellular lipid droplets that aids in regulating lipid packaging. Various normal lipid-laden cells (e.g., adrenal zona fasciulata, Sertoli cells, glandular breast tissue, steatotic hepatocytes, sebocytes and some macrophages) express adipophilin while mature adipocytes do not. Adipophilin expression has diagnostic efficacy in lipid-rich neoplasms such sebaceous carcinomas. Since lipomatous tumors variably contain lipoblasts (cells with lipid-rich droplets), we examined adipophilin expression in various lipomatous tumors and undifferentiated pleomorphic sarcomas (UPS).
Design: 43 lipomatous tumors including liposarcomas [myxoid liposarcoma (MLS), n=8; pleomorphic liposarcoma (PLS), n=5; well differentiated liposarcoma (WDLS), n=10; dedifferentiated liposarcoma (DLS), n=10] and lipomas [conventional, n=5; hibernoma n=2; spindle cell lipoma (SCL) n=2; pleomorphic lipoma (PL) n=1] and 9 UPS with FFPE tissue were retrieved from institutional pathology files and labeled with adipophilin antibody (predilute, AP125, Fitzgerald Industries, Concord, MA). The labeling intensity, pattern and percent tumor involvement were recorded. Labeling patterns were (1) vesicular: variably-sized intracellular vesicles, often in lipoblasts; (2) membranous: adipocytic cell membranes and (3) granular: small round to irregular cytoplasmic inclusions.
Results: All 5 PLS demonstrated predominantly vesicular labeling (2-3+ intensity, 5-95% of tumor cells). 5 of 8 MLS (1-2+ intensity, 5% to >95% of tumor cells) and 4 WDLS (1-3+, 5%) had vesicular and membranous labeling while only 1 DLS had focal vesicular labeling with most DLS having granular labeling. Lipoblasts in all liposarcoma types invariably showed vesicular staining. 1 of 5 conventional lipomas and 1 of 2 SCL demonstrated focal(1%, 1-2+) membranous pattern. The PL and hibernoma showed diffuse labeling(>90%, 2-3+ with vesicular and membranous patterns). All UPS showed variable labeling(<5-90%, 1-2+) with prominent granular patterns.
Conclusions: Adipophilin antibodies label lipid droplets and lipoblasts (vesicular pattern) in some lipomatous tumors including PLS, MLS, WDLS, PL and hibernomas. Tumors with mature white adipocytes did not show vesicular labeling. The vast majority of UPS have adipophilin reactivity but with less intensity and prominent granular pattern in contrast to adipocytic neoplasms. Adipophilin may be a useful ancillary tool to detect lipoblasts in sarcomas, but appreciation of staining patterns is critical.

1957 The Use of Multispectral Imaging in Fine Needle Aspiration Biopsies of Reactive Lymphoid Hyperplasia and Follicular Lymphoma

A Zarineh, J Yu, RE Felgar, WE Khalbuss, K Cieply, SE Monaco. University of Pittsburgh Medical Center, Pittsburgh, PA.
Background: The cytologic distinction between reactive lymphoid hyperplasia (RLH) and small cell lymphomas, such as follicular lymphoma (FL), can be difficult in fine needle aspirations (FNA). The use of ancillary tests in these cases is crucial, and often includes flow cytometry (FC), immunohistochemistry (IHC), and fluorescence in-situ hybridization (FISH). The interpretation of IHC can be challenging due to the subjective and qualitative nature, in addition to the need for multiple sections for analysis of multiple antibodies. Multispectral imaging (MSI) with quantum dots involves highly fluorescent molecules that allow multiple spectra to be distinguished when used in combination, which allows for more precise signal quantitation. Thus, we examined the ability of MSI to provide quantitative and useful data to help in distinguishing RLH and FL in FNA biopsies.
Design: A total of 8 FNA cell block sections from 4 RLH and 4 FL cases were stained using immunohistochemical stains (CD3, CD20, CD10, and bcl-2) conjugated to quantum dot fluorophores. A series of slides were also used for controls and for creating a spectral library on the Nuance CRI Flex microscopy system (CRi, Cambridge Research & Instrumentation, Woburn, MA; spectral range 420 to 720 nm). A total of 3 fields of view (FOV) at 10x magnification were captured for each case and analyzed using the Nuance software version 2.10.
Results: All 8 cases were from FNAs of lymph nodes (4 FNA performed by pathologist, 2 CT-guided, 2 US-guided). The analysis of the 24 FOV revealed that the FL cases tended to show more CD20-positive cells than CD3-positive cells (lower CD3:CD20 ratio; 0.3 vs. 3.9), and tended to have more pixels colocalizing CD20/CD10/bcl-2. For quality control purposes, the average percent of pixels colocalizing CD3 and CD20 was less than 0.4%.

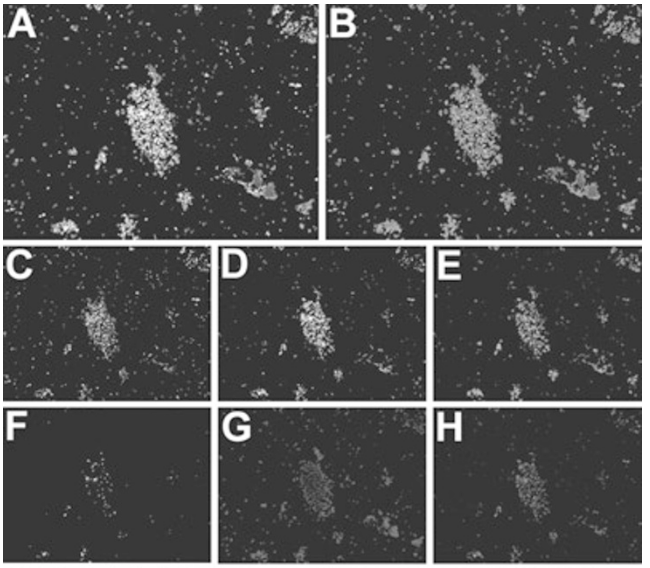

FIGURE : A cell block section from an FNA case of follicular lymphoma where four antibodies labeled with QDs were utilized to demonstrate the ability to do multispectral imaging on a single cell block (10x objective magnification). The four antibodies included: CD20 (yellow; C), CD10 (green; D), bcl-2 (magenta; E), and CD3 (aqua; F). In addition, DAPI was used to stain all nuclei (G). The image in A shows the composite image with signals from all four antibodies, while the smaller images (C through H) show the same image unmixed for each separate antibody. The red signal in figure B and H indicates the colocalization of cells positive for CD20/CD10/bcl-2. There appears to be a lymphoid follicle in the center with a high concentration of CD20/CD10/bcl-2 positive cells (red signal; B and H), indicating a neoplastic population, consistent with follicular lymphoma. Non-neoplastic germinal center cells can be CD20 and CD10 positive, but should not express bcl-2.

Conclusions: This study shows that MSI is feasible on FNA cell block material and can be helpful in obtaining quantitative data from multiple antibodies used on a single slide, which may be advantageous in FNA samples with limited material and may potentially be helpful in the cytologic distinction of RLH and FL.

1958 Automated Brightfield Dual Color In Situ Hybridization for Detection of *MDM2* Gene Amplification in Sarcomas

W Zhang, A McElhinny, A Nielsen, M Wang, M Miller, S Singh, R Rueger, B Rubin, RR Tubbs, P Roche, P Wu, L Pestic-Dragovich. Ventana Medical Systems, Inc., Tucson, AR; Roche Diagnostics GmbH, Penzberg, Germany; Cleveland Clinic, Cleveland, OH.

Background: The human homologue of the mouse double minute 2 (*MDM2*) oncogene is amplified in about 20% of sarcomas. Measurement of *MDM2* amplification can aid in classification, and may provide predictive value for recently formulated therapies targeting *MDM2*. Here, we have developed and validated an automated brightfield dual color *in situ* hybridization application for *MDM2* gene amplification in sarcomas.

Design: A repeat-depleted *MDM2* probe was constructed to target the *MDM2* gene region at 12q15. A chromosome 12-specific probe (Chr 12) was generated from pα12H8 plasmid. The ISH assay was developed with dinitrophenyl-labeled *MDM2* probe and digoxigenin-labeled Chr 12 probe on Ventana Medical Systems, Inc. automated slide staining platforms. The specificity of the *MDM2* and Chr 12 probes was demonstrated on metaphase spreads, and further validated against controls including normal human tonsil and known *MDM2*-amplified samples. The assay performance was evaluated on a cohort of 68 FFPE specimens using a conventional brightfield microscope.

Results: Simultaneous hybridization and signal detection for *MDM2* and Chr 12 demonstrated both DNA targets in the same cells. 66 of 68 cases had interpretable signals for *MDM2* and Chr 12. While all four lipomas were nonamplified and eusomic, *MDM2* amplification was noted in 81% (21/26) of well-differentiated liposarcomas. *MDM2* amplification was observed in 1 of 8 osteosarcomas; 3 demonstrated Chr 12 aneusomy; and the other 4 were non-amplified. *MDM2* amplification was present in 1 of 4 chondrosarcomas; the remaining 3 cases had normal *MDM2* and Chr 12 copy numbers. 11 of 13 synovial sarcomas displayed no evidence of *MDM2* amplification on most cells; the other two had Chr 12 aneusomy. In pleomorphic sarcoma, not otherwise specified (malignant fibrous histiocytoma), *MDM2* was amplified in 31% (4/12) interpretable cases, while 92% (11/12) were aneusomy for Chr 12 . One alveolar rhabdomyosarcoma and two embryonal rhabdomyosarcoma cases had low level aneusomy of Chr 12.

Conclusions: The use of ISH *MDM2*/Chr 12 assay allows the simultaneous analyses of the two DNA targets within the context of tissue morphology. This method combines the advantage of brightfield microscopy with fully automated analysis and has the potential for routine application in surgical pathology.

Ultrastructural

1959 Electron Microscopic Finding in Skin Biopsies from Patients with Danon Disease

J Alroy, R Pfannl, D Slavov, MRG Taylor. Tufts University School of Medicine, Boston, MA; Tufts Cumming's School of Veterinary Medicine, Grafton, MA; Tufts Medical Center, Boston, MA; University of Colorado, Aurora, CO.

Background: Danon Disease is an X-linked lysosomal storage disease. It is due to primary deficiency of lysosomal-associated membrane protein-2 (LAMP-2). LAMP-2 is an important regulator of maturation of both autophagosomes and phagosomes. Deficiency of LAMP-2 results in accumulation of autophagosomes in multiple tissues and a phenotype triad of hypertrophic cardiomyopathy, myopathy, and mental retardation. A milder phenotype occurs in females. Clinical manifestation typically develops in boys in the first two decades of life. Skin biopsy is a useful cost effective tool for the diagnosis of other lysosomal storage diseases, but its role in Danon disease has not been studied.

Design: In this study we obtained skin biopsies from the forearms of a 24-years- old man and a 43-years-old woman and her 9-year-old son from two unrelated families. The diagnosis of Danon diseases was confirmed by DNA analysis and absent LAMP-2 protein in skin fibroblasts from both males. The 2-mm^2 biopsies were fixed in Trump's fixative and postfixed in 1% osmium tetroxide in sodium cacodylate buffer, stained with 5% uranyl acetate, dehydrated and embedded in resin (Epon-812). Thick sections (1um) were stained with toluidine blue. Thin sections were cut at 50-70nm, stained with uranyl acetate and lead citrate, and photographed with a transmission electron microscope.

Results: Few large membrane bound electron lucent vacuoles, i.e., lysosomes were noted in myelinated axons and in some smooth muscle and fewer in perineural cells. Some fibroblasts contain both electron lucent lysosomes as well as lysosomes that contain electron dense material. Rare storage of lamellated membrane structures was noted in unmyelinated axons.

Conclusions: These unique morphological findings demonstrate the usefulness of skin biopsies in the diagnosis of Danon disease. They are distinct from those seen in patients with muscopolysaccharidosis, with glycolipids and oligosacchardide storage diseases, neuronal ceroid lipofuscinosis, as well as various myopathies.

1960 Birt-Hogg-Dubé Renal Tumors Express Characteristic Ultrastructural Features Which Distinguish Them from Other Hereditary and Sporadic Renal Neoplasms

S Hebert-Magee, MJ Merino, WM Linehan, M Tsokos. National Institutes of Health, Bethesda, MD.

Background: Birt-Hogg-Dubé (BHD) syndrome is an autosomal dominant genodermatosis characterized by a predisposition to hamartomatous cutaneous lesions, spontaneous pneumothoraces, pulmonary cysts and renal neoplasms. Light microscopic evaluation of the BHD renal tumors has suggested the existence of various morphologies including chromophobe, oncocytic and hybrid variants. To date, there has been no ultrastructural analysis of these tumors.

Design: We utilized the collection of BHD renal neoplasms at our institution and evaluated their ultrastructural features in comparison to those of sporadic or familial chromophobe carcinomas and oncocytomas. Eleven cases were evaluated, 5 of which BHD associated and 6 sporadic or familial.

Results: We found that all 5 BHD renal tumors expressed a hybrid chromophobe/oncocytic phenotype, which was apparent in individual tumor cells. Specifically, tumor cells exhibited numerous mitochondria (oncocytic phenotype) and microvesicles (chromophobe phenotype). The mitochondria were similar to those described in sporadic oncocytomas, i.e. small and round with lamellar cristae. Many tumors contained cells with apical villi and formation of lumina and with elaborate cytoplasmic interdigitations. Sporadic or familial tumors without BHD mutation were of pure morphology, either oncocytic (5 tumors), or chromophobe (1 tumor). The chromophobe tumor also had many mitochondria, but they were of variable size including large ones and had the characteristic tubulovesicular cristae. Luminal differentiation was present in the chromophobe carcinoma, but not in the oncocytomas. All but one oncocytomas had focal intracytoplasmic aggregates of filaments and consisted of groups of cells surrounded by thick basement membrane. The cytoplasmic contours were smooth, except in one tumor, which showed basal interdigitations. Lipid droplets and glycogen were present but not abundant in all tumors.

Conclusions: Our study showed that all BHD renal tumors exhibit a hybrid chromophobe/oncocytic ultrastructural phenotype, which distinguishes them from oncocytic or chromophobe tumors in sporadic or other familial settings. Therefore, electron microscopy can be instrumental in identifying BHD patients without overt clinical manifestations.

1961 Fulminant Hepatic Failure and Giant Cell Hepatitis Associated with Paramyxoviral-Like Inclusions: Contribution of Electron Microscopy

J Hicks, SH Zhu, J Barrish. Texas Children's Hospital & Baylor College of Medicine, Houston, TX.

Background: Etiologic agents responsible for acute fulminant liver failure (AFLF) and giant cell hepatitis (GCH) are not readily identified. Paramyxovirus (PV) has been associated with AFLF and GCH in children and adults (NEJM 1991;324:455; UltraPath 2001;25:65). PV hepatitis is associated with giant cell transformation, cholestasis, bridging fibrosis, chronic hepatitis, and rapidly progressive fulminant liver disease. Time-consuming viral cultures may detect PV in some, but not all cases. PV PCR is not currently available. PV inclusions may be identified based upon ultrastructural features.

Design: 7 children with GCH and/or AFLF were studied (5M:2F, age range 6wks-11yrs, mean 7yrs). Liver biopsies and/or explants were available for evaluation. Tissue was submitted for viral cultures and viral PCR studies, and also available for routine and electron microscopic study. Histopathologic examination included H&E, PAS, PAS with diastase, trichrome, iron and copper staining. Immunocytochemistry for Adenovirus, CMV, HSV, EBV, Parvovirus and Hepatitis B were performed with most cases. Electron microscopy was performed.

Results: Liver biopsies and explants demonstrated giant cell transformation, ballooning degeneration, binucleate hepatocytes, cytoplasmic and canalicular cholestasis, pseudoacinar formation, and reactive and pyknotic nuclei. Occasional hepatocytes had eosinophilic glassine cytoplasm. There were frequent apoptotic hepatocytes and geographic necrosis. Chronic inflammatory infiltrates with only infrequent acute inflammatory cells were present. Immunocytochemistry failed to identify Adenovirus, CMV, HSV, EBV, Parvovirus and Hepatitis B. Electron microscopy identified viral inclusions within the cytoplasm of occasional hepatocytes. The viral inclusions were comprised of relatively large round to ovoid aggregates of fine filamentous, beaded substructures (14-20 nm width). Viral inclusions were interspersed with typical cell organelles. There were no intranuclear inclusions. The ultrastructural features are those associated with paramyxovirus. 4 cases subsequently had paramyxovirus identified by viral cultures.

Conclusions: Paramyxovirus is associated with an aggressive clinical course and rapidly progressive AFLF. Ultrastructural examination of liver biopsies/explants with GCH and AFLF may allow for identification of ultrastructural features of paramyxovirus as the etiologic agent, aid in clinical management, and assist in determination of prognosis.

1962 Ultrastructural Features of Gelophyisic Dysplasia: Role of Electron Microscopy in Diagnosis

J Hicks, JP Barrish, SH Zhu, N Brunetti-Pierri. Texas Children's Hospital & Baylor College of Medicine, Houston, TX; Baylor College of Medicine, Houston, TX.

Background: Geleophysic Dysplasia (GD), an autosomal recessive disorder, is a member of the Acromelic Dysplasia Group, which includes Weill-Marchesani Syndrome and Acromicric Dysplasia. All 3 disorders are characterized by short stature, short hands, stiff joints, delayed bone age, cone-shaped epiphyses, thick skin and heart disease. Molecular testing is in the development phase and of considerable expense. GD is a lysosomal storage disease that may be identified by electron microscopy of cultured fibroblasts.

Design: 8 children with clinically suspected GD underwent skin punch biopsies to establish fibroblast cultures for electron microscopic examination, and for future genetic and molecular testing. The study population consisted of 5 males and 3 females with an age range from 13 months to 13 years. Fibroblasts were harvested from the cell cultures, and prepared for electron microscopic examination. 4 skin cell cultures of normal fibroblasts were examined as controls.

Results: Light microscopic examination of the semi-thin sections of the cultured normal and GD fibroblasts showed cellular specimens. The fibroblasts were round to ovoid in outline and had a moderate amount of cytoplasm. The nuclei tended to have indented